THE INFLUENCE OF TURBULENCE ON DUST AND GAS EXPLOSIONS IN CLOSED VESSELS

by

Jean-François Bond

McGill University, Montreal

September 1985

A Thesis Submitted to the Faculty of Graduate Studies and Research in Partial Fulfillment of the Requirements for the Degree of Master of Engineering

ISBN - 0-315-34450-4

ABSTRACT

Experiments have been carried out to assess the influence of turbulence on the burning rate of cornstarch-air explosions in closed vessels. Different means of varying the turbulence were used, so as to investigate a substantial range of turbulence intensity and a variety of turbulent flow structures.

Since gas-air deflagrations are currently better understood than dust-air deflagrations, all experiments done with the cornstarch-air mixture were replicated with a methane-air mixture, in order to compare the influence of turbulence in explosions in the two media.

The most important finding of the study was that the ratio of the burning rate of the gas-air mixture to that of the dust-air mixture, observed under identical conditions of turbulence, was a constant, independent of the intensity of the turbulence and of the details of the structure of the turbulent flow. This suggests that this ratio is a function of the physico-chemical properties of the mixtures themselves.

RESUME

La présente étude a eu pour objet d'évaluer l'influence de la turbulence sur le taux de combustion d'une explosion se propageant dans un mélange amidon-air contenu dans une enceinte fermée. Dans ce but, nous avons utilisé diverses méthodes de génération de la turbulence afin d'en modifier la structure et de faire varier son intensité.

Les déflagrations dans les mélanges biphasiques étant moins bien connues que celles dans les mélanges gazeux, toutes les expériences réalisées avec le mélange amidon-air ont été reprises avec un mélange méthane-air, afin de comparer l'influence de la turbulence sur des explosions se produisant dans ces deux milieux. Cette étude comparative nous a permis de montrer que le rapport du taux de combustion du mélange gazeux sur celui du mélange biphasique mesurés dans les mêmes conditions expérimentales est constant. Il semble donc que ce rapport ne dépende ni de l'intensité de la turbulence, ni de sa structure, mais uniquement des propriétés physico-chimiques des mélanges eux-mêmes.

ACKNOWLEDGEMENTS

The author would like to gratefully acknowledge the constant help and guidance of Professors J.H.S. Lee and R. Knystautas who initiated this study and supervised its progress.

The invaluable contributions of Mr. Marc Champagne, in building electronic instrumentation, and of Messrs. Moris Fresko and Aris Makris, in performing some of the experimental work, are acknowledged with deep gratitude.

The author is also thankful for the many stimulating discussions on dust combustion provided by his colleagues Mrs. Yi Kang Pu, Mr. Neil Craft, Mr. Panayiotis Theofanous, Mr. Michael Gaug and Mr. Olivier Peraldi.

Last, but not least, the author would like to thank his parents for their constant encouragement and support during the course of this degree.

TABLE OF CONTENTS

i- NOMENCLATURE

A	Area
D	Diameter
E	Energy
Ge	Turbulence decay number —
K	Normalized burning rate
K'	Ratio of normalized burning rate to a reference value
M	Mass
P	Pressure
R	Universal gas constant
Re	Reynolds number
S	Burning velocity
T	Temperature
U	Internal energy
V	Volume
c	Specific heat
g	Acceleration of gravity
k	Thermal conductivity
l	Integral length scale of turbulence
m	Mass
r	Radius
u	Velocity or speed
u'	Turbulent r.m.s. velocity
γ	Specific heat ratio of gaseous mixture
$\bar{\gamma}$	Specific heat ratio of dust-air mixture
Δ	Difference
δ	Flame thickness
ε	Turbulence kinetic energy decay rate
ε'	Eddy diffusivity
η	Kolmogoroff microscale of turbulence
θ	Half-energy time of turbulence decay
κ	Ratio of dust mass to gas mass per unit volume of mixture
λ	Taylor microscale of turbulence
μ	Dynamic viscosity
ν	Kinematic viscosity
ρ	Density
τ	Characteristic time

Subscripts

a	Activation
b	Dispersion bottle
c	Combustion chamber
d	Developed
de	Decay
dev	Devolatilization
e	Enclosed
f	Final
g	Gas
i	Initial
l	Laminar
o	Reference
p	Constant pressure
set	Settling
st	Dust (staub)

t	Turbulent
u	Unburned
v	Constant volume
vr	Velocity rise
tr	Temperature rise

I- INTRODUCTION

a) Introductory remarks

All situations of practical interest in the combustion of dust-air mixtures involve a certain degree of turbulence. In pulverized coal burners, the coal-air mixture enters the burner as a turbulent jet, and additional means of inducing turbulence are often used to enhance the burning rate[1]. In a typical grain silo explosion, the initial ignition of a small dust-air pocket creates a flow field which raises more dust into suspension, and subsequent flame propagation takes place in this turbulent mixture[2]. Hence turbulence is an intrinsic feature of a dust explosion, and the study of the influence of turbulence on the burning rate of a dust-air mixture in an important area of dust combustion research.

An adequate understanding of the influence of turbulence on the burning rate of dust-air mixtures is especially important to those who are concerned with safety in coal mines, grain silos, and industrial process equipment where dust is handled. The proper design of explosion relief vents for grain silos, for example, requires an estimate of the maximum rate of pressure rise associated with the dust explosion. This type of problem has received considerable attention since the series of grain elevator explosions in the United States, in December 1977[3].

Renewed interest in the design of internal combustion engines fueled by coal dust is another subject for which a knowledge of the role played by turbulence could be of high importance[4]. A fair amount of research has been done on these

engines in recent years and it appears at present that the burning rates achieved are too low to permit the construction of an engine with a r.p.m. sufficiently high for practical applications. Hence an understanding of the means by which increases in burning rates may be achieved is critical to further progress in this field.

In attacking the complex problem of dust explosion, it is wise to try to draw upon our knowledge of gas and vapor phase explosion. For homogeneous gases and vapors, the fundamental parameters that characterize the explosibility of a mixture (e.g. minimum ignition energy, laminar burning velocity, flammability limits, etc.) are well known and their value can be measured directly by experiments. The effects of turbulence on the propagation of a gas-air flame are also fairly well established, at least on a qualitative basis[5], and there exists enough reliable experimental data to permit engineering estimates of the burning rate under different flow conditions. By contrast, no reliable fundamental parameters are as yet known for explosive dust-air mixtures. Hence the study of gas explosion in conjunction with dust explosion under the same conditions can help elucidate the structure and propagation mechanisms of dust-air flames. In particular, it is worthwhile to compare the effect of turbulence on dust-air explosions to that on gas-air explosions occurring in the same apparatus, with identical flow fields. Such a comparison is the program of this thesis.

It is generally known that turbulence plays a strong role in the development of a dust-air explosion. As yet, however, the few experimental studies that have been performed have not

yielded empirical relationships linking the burning rate to the relevant parameters of the turbulence. One reason for this is that it is difficult to define turbulence in the context of a closed vessel explosion without mean flow, and that measurement of fluctuating velocities in a dust-air suspension poses important experimental problems. Furthermore, even if one measures the flow velocity at a given point in the combustion chamber prior to ignition, compression of the unburned mixture and irregular fluid motions caused by the flame itself start to change this velocity as soon as the flame ball begins to propagate towards the walls of the vessel - it is therefore doubtful that such a measurement is of any value.

For these reasons, it was thought worthwhile to perform some rather crude experiments to investigate the influence of "turbulence" on the maximum burning rate of explosions inside closed vessels. "Turbulence", in the context of this thesis, will be taken to refer to any fluid motion in the combustible mixture, and the intensity of the turbulence will be characterized by the value of a relevant parameter of the device used to generate the fluid motions.

The experiments whose results are reported in this thesis were carried out in two vessels of similar dimensions: a 333 liter sphere and a 180 liter vertical cylinder with a height to diameter ratio of two. Cornstarch, an organic polymer with 100% volatile content, was used as fuel in all the dust experiments; a 7.5% methane-air mixture, whose energetics are similar to those of the starch-air mixture, was used in all the gas experiments. The experiments focussed on assessing how the initial flow field of the explosive mixture affected the

maximum pressure developed, which is a measure of the extent of the reaction, and the maximum rate of pressure rise, which is a measure of the rate of the reaction.

b) Outline of the thesis

The thesis begins by a discussion of the physical mechanisms that are thought to be relevant to the propagation of turbulent explosion flames and a review of the previous work that has been done in the area of turbulent dust and gas explosions (chapter 2). Such a discussion provides the necessary framework for the proper interpretation of all experimental results.

Chapter 3 describes the details of the apparatus and of the experimental procedures. The results of a preliminary series of experiments, in which the variation of maximum pressure (P_{max}) and maximum rate of pressure rise $(dP/dt)_{max}$ with cornstarch concentration was measured, are also presented in this chapter and are found to be in good agreement with those reported by other workers. This serves to establish some confidence in the quality of the apparatus and of the experimental method.

In chapter 4, the results of experiments measuring the effect of dispersion-induced turbulence are presented. Dispersion of the dust was achieved by an air blast from a small bottle charged to high pressure, directed at a dust bowl at the center of the vessel. Hence some turbulence is associated with the dispersion process itself and the features of this turbulence can be varied by adjusting either the initial pressure of the dispersion bottle or the delay between

dispersion of the dust and ignition of the mixture. In this chapter it is seen that the burning rate of dust and gas respond to dispersion pressure variations in a similar manner, but that for a given dispersion pressure, the burning rate of a dust-air mixture decreases faster with ignition delay than does that of a gas-air mixture. Some possible explanations to this discrepancy are introduced.

Chapter 5 describes the results of experiments measuring the effect of jet-induced turbulence on dust and gas explosions in the 333 liter sphere. Additionnal turbulence of controllable intensity was introduced in the sphere by a series of air jets along a circular ring or along a vertical tube. In this case, the burning rate increases observed with the dust-air mixture are nearly equal to those obtained with the gas-air mixture.

The results of the study suggest that the ratio of the turbulent burning rates of mixtures of dust-air and gas-air observed under identical conditions of turbulence is not sensitive to differences in the detailed structure of the turbulence induced by the various devices used to generate it, but that it rather depends on the physico-chemical properties of the mixtures themselves. This idea is elaborated on in the concluding chapter (chapter 6), where some suggestions about useful future work on this subject are also made.

II- RELEVANT PHYSICAL MECHANISMS AND REVIEW OF PREVIOUS RESEARCH

To put the experimental results obtained in this study in the proper perspective, it is necessary to first establish a framework of the physical mechanisms which are thought to influence the propagation of a turbulent flame. This is the primary purpose of this chapter.

Some comments on the nature of homogeneous turbulence will first be introduced. A brief discussion of the mechanisms of flame folding and turbulent eddy transport will follow. This discussion will allow us to determine the length, time and velocity scales that are involved in the consideration of the burning rate. It will then be possible to compare, in a qualitative manner, the burning rate increases expected to follow from a given turbulence in gas-air flames and dust-air flames.

The Bradley-Mitc' son[6] model of explosion development in a spherical vessel, relating the experimentally observable values of pressure, rate of pressure rise and burnout time to the fundamental burning velocity of the mixture and the radius of the vessel, will be introduced and its validity will be assessed in the context of our experimental conditions. It will be seen that while the turbulent flame structure observed in our experiments is more complex than that assumed in the Bradley-Mitcheson model, the model is still of some use in converting tha apparatus-dependent value of maximum rate of pressure rise $(dP/dt)_{max}$ to the standard quantity of turbulent burning velocity (S_t), which can be compared to that of other

researchers.

Finally, a brief review of the existing experimental work on turbulent dust and gas explosions will be made.

a) Turbulence and turbulent combustion

Turbulence, a random-like, disorganized flow pattern with a complex underlying structure, is usually studied in contexts where a mean flow can be identified, such as in jets, wakes or boundary layers. In these situations, it is natural to consider the flow velocity u to be made up of a time-averaged value $\bar{u}$, representing the mean flow at that point, plus a fluctuating quantity u', representing "turbulence". Because the equations governing the behavior of these fluctuations are outnumbered by the flow variables (closure problem), a complete mathematical description of turbulent fluid flow appears beyond reach. Hence to represent the phenomenon of turbulence for practical applications, a simplified physical model must be introduced.

A particularly fruitful line of thought, in the elaboration of such a model, is the consideration of the kinetic energy associated with the turbulent fluctuations. Consider, for example, the useful idealization of homogeneous, isotropic turbulence. On the macroscopically observable scale, this turbulence appears to consist in a collection of "eddies" or swirls, with characteristic length l and characteristic velocity u', which decay, or disappear, in time of the order of l/u' [7]. For steadiness, the rate of supply of energy from the mean flow to the fluctuating motions must equal the rate of decay of the energy associated with the large eddies. The order of magnitude of this rate is simply the kinetic energy per unit

mass of eddy (u'^2) divided by the eddy lifetime (l/u'):

$$\varepsilon = \frac{u'^2 u'}{l} = \frac{u'^3}{l} \tag{1}$$

The energy that "disappears" with the decay of the large eddies must either be recovered as kinetic energy of smaller scale motions, or be dissipated as thermal energy by viscous shear. The rate of energy dissipation by viscous shear that occurs on the length scale of the macroscopic eddies is simply estimated as the product of the viscous shear stress on a unit volume of fluid ($\frac{\mu u'}{l}$) times the strain rate (u'/l) divided by the mass of the volume (ρ):

$$\frac{\mu u'}{l} \frac{u'}{l} \frac{1}{\rho} = \frac{\mu u'^2}{\rho l^2} \tag{2}$$

The ratio of the rate of energy supply to that of viscous dissipation occurring at the macroscale level is, therefore,

$$\left[\frac{u'}{l}\right]^3 \frac{\rho l^2}{\mu u'^2} = \frac{u' l}{\nu} \equiv Re \tag{3}$$

Since in turbulent flow, Re is a very large number (typically, $Re > 10^3$), no significant dissipation takes place on the macroscopic scale: the energy is transfered to smaller scale motions through a cascading process that ends when the length scale of these motions is sufficiently small for viscous dissipation to be effective in converting organized motion into random, thermal motion. It follows from the above discussion that the length and velocity scale of the dissipative regions must be related to their characteristic dissipation rate by

(4) $\varepsilon_\eta = u_\eta^3/\eta = \nu(u_\eta/\eta)^2$ or (5) $\eta = (\nu^3/\varepsilon_\eta)^{\frac{1}{4}}$, (6) $u_\eta = (\nu\varepsilon_\eta)^{\frac{1}{4}}$

where η is called the Kolmogoroff scale.

On the basis of these arguments, and taking into account the experimentally observed fact, that viscous dissipation in turbulence is intermittent, i.e. occurs only in highly localized regions scattered throughout the flow, Tennekes[8] has proposed the following simplified model of turbulence. Turbulence consists in macroscopic swirls with a velocity of the order of the turbulent r.m.s. velocity and length scale of the order of the integral length scale, on which are superimposed dissipative vortex tubes with a diameter of the order of the Kolmogoroff microscale η and a spacing of the order of the Taylor microscale λ, i.e. a scale which relates the rate of turbulent kinetic energy dissipation per unit mass to the turbulent r.m.s. velocity. The model is depicted in figure 1, where we have also represented other length scales that are important in turbulent dust flame propagation along with the order of magnitude of these length scales as they occur typically in explosions of the type considered in this study.

The Tennekes model has been widely accepted in recent efforts to observe and model turbulent flame propagation, for example by Tabaczynski et al[9-11], Ohta[12], and Chomiak[13]. In the context of the Tennekes model, we now discuss the two physical mechanisms that are deemed responsible, in the current theories of turbulent flame propagation, for the burning rate increase due to turbulence: flame wrinkling and turbulent eddy transport.

Irregular wrinkling of the flame front because of velocity fluctuations in the flow field directly ahead of the flame

causes an increase in the total burning area, and hence in the burning rate. Insofar as the laminar burning velocity of the mixture is not affected by the wrinkling process, the ratio of turbulent burning velocity to laminar burning velocity in wrinkled laminar flame propagation is simply given by

$$\frac{S_t}{S_l} = \frac{A_d}{A_e} \tag{7}$$

where A_d and A_e refer to the developed and enclosed flame areas, respectively. It stands to reason that the characteristic spacing of the flame wrinkles should be related to the integral length scale, and that the magnitude of the wrinkles should depend on the turbulent r.m.s. velocity, u'. Hence wrinkled laminar flame theories yield predictions of turbulent burning velocity in terms of the macroscopic features of the turbulence: $S_t = S_t\ (S_l, u', l)$. Velocity fluctuations on the microscopic scale, on the other hand, play an important role in the energy and mass transport processes inside the flame itself. If these fluctuations are significant, then the mechanism determining the rate of propagation of the flame front normal to itself is no longer molecular diffusion, but rather turbulent eddy transport. Damkohler[14] was the first to propose a theory of turbulent flame propagation based on turbulent eddy transport. Since thermal flame theory shows that laminar burning velocity is proportional to the square root of the diffusivity of the medium, Damkohler concluded that

$$S_t/S_l = (\varepsilon'/\nu)^{\frac{1}{2}} \tag{8}$$

where ε' is the eddy diffusivity of the turbulent flow field.

Recent models of turbulent flame propagation, such as the two-eddy theory of Abdel-Gayed and Bradley [15], have recognized that both of the abovementionned mechanisms play an important role in enhancing the burning rate. However, it is easy to see that the relative importance of the two mechanisms will depend critically on the relationship between the relevant chemical scales of the mixture on the one hand, and the fluid mechanical scales of the turbulence, on the other hand [16].

If the laminar flame thickness δ is smaller than the scale of the smallest turbulent fluctuations η, then turbulent eddy transport inside the flame is impossible and flame wrinkling alone is responsible for turbulent burning rate increase. If, on the other hand, the flame thickness spans many Kolmogoroff eddies, while being less than the integral scale, the two processes of turbulent burning rate increase will be important. Finally, if the flame is as thick as the characteristic dimension of the macroscopic turbulence, then wrinkling by the large eddies can only have a minimal impact on total burning rate, and only turbulent eddy transport can play a significant role. Hence, to predict the influence of turbulence on dust and gas explosions under the same experimental conditions, it is necessary to have some idea of their laminar flame thickness. The thickness of laminar gas-air flames has been the subject of extensive studies [17] and it is agreed that this thickness, measured as the depth of the temperature profile, varies in orders of magnitude between 10^{-4} and 10^{-3} m. By contrast, very little research has been done with laminar dust-air flames, partly owing to the difficulties in achieving a stable, laminar dust-air suspension for burner studies. Smoot [18] reports laminar

coal-dust-air flames with a thickness of 10^{-2} m, while measurements of quenching distance performed by Mason and Wilson[19] indicate a thickness of approximately 3×10^{-3} m for a flame of lycopodium spores, a vegetable dust whose structure is probably similar to that of cornstarch. Hence a cornstarch flame is probably not a lot thicker than a methane-air flame, and this may imply that turbulence will have a similar effect on cornstarch-air and methane-air explosions. However, it must be stressed that this argument is highly speculative, since no study of the laminar flame structure of cornstarch-air mixtures has ever been done.

b) Review of constant volume explosion theory

In a closed vessel explosion, a centrally ignited flame propagates outward towards the walls of the vessel and combustion of the mixture results in final overpressure ratios typically of the order of 6 to 10.

Pressure measurements of dust explosion experiments performed in closed vessels allow us to obtain an estimate of the extent of the burning (from the maximum pressure developed, P_{max}) and of the rate of combustion (from the maximum rate of pressure rise, dP/dt_{max}). Models of explosive combustion in a closed vessel show that the burning velocity S, the pressure P and the rate of pressure rise dP/dt are related to each other in a simple manner. It is of interest to use the results of pressure measurements to obtain the burning velocity, because this quantity can serve as a basis for comparing our data with those obtained by other researchers in a variety of

experimental set-ups. Bradley and Mitcheson[6] have recently reviewed the problem of spherical vessel explosion and concluded that a very good approximate, analytical solution to the pressure development can be derived with the help of a few simplifying assumptions. The most important assumptions are the following:

1- Regular, spherical flame propagation without heat loss.

2- The burned and unburned mixtures behave as perfect gases.

3- The unburned mixture is being compressed isentropically by the propagating flame.

4- The pressure rise is directly proportional to the mass fraction burned.

The burning velocity formula obtained from these assumptions is

$$S = \frac{\frac{dP}{dt}}{\frac{3}{r}\left[\frac{P}{P_i}\right]^{1/\gamma_u}(P_f - P_i)\left[1 - \left[\frac{P_i}{P}\right]^{1/\gamma_u}\left(\frac{P_f - P}{P_f - P_i}\right)\right]^{2/3}} \tag{9}$$

where P = Pressure

P_i = Initial pressure

P_f = Final explosion pressure

S = Burning velocity

r = Vessel radius

γ_u = Specific heat ratio of the unburned mixture.

From the above expression, the maximum rate of pressure rise is obtained when

$$P = P_f \tag{10}$$

i.e. at the very end of the flame travel. This stands to reason, because the last shell of fuel-air mixture of thickness Δr that burns, has the biggest volume and the highest density of all such shells. Furthermore, as P approaches P_f, the rate of pressure rise is related to the scale of the vessel by

$$(11) \qquad \frac{dP}{dt} = \left(\frac{dP}{dt}\right)_{max} = \frac{3}{r}(P_f - P_i)\, S$$

Hence the maximum rate of pressure rise in two vessels with radiuses r_1 and r_2, and with identical burning velocity and final and initial pressure, should be related by

$$(12) \qquad \left(\frac{dP}{dt}\right)_{max\ 1} r_1 = \left(\frac{dP}{dt}\right)_{max\ 2} r_2 = \text{constant}$$

Bartknecht[20] has found experimentally a scaling law applicable to the burning of many dust-air and gas-air mixtures in vessels of different sizes and shapes:

$$(13) \qquad \left(\frac{dP}{dt}\right)_{max} V^{1/3} = K_{st}$$

where V is the vessel volume and K_{st} is a constant of the dust-air mixture (st stands for "staub", which is german for dust. The term K_g is used when a gas mixture is being considered). This law reduces to equation 11 in the case of a spherical vessel. Equation 11 also makes clear that the maximum rate of pressure rise is directly proportional to the burning velocity.

Out of all the assumptions made in the Bradley-Mitcheson model, that of regular, spherical flame propagation without

heat loss is probably the one that is least satisfied in the experimental conditions of this study. As we have seen before, a turbulent flame front is wrinkled by the turbulent velocity fluctuations and this wrinkling can be so severe as to create a situation, such as has been observed by Shchelkin [21] in circular tubes, where pockets of unburned mixture are left behind the propagating flame front. Such a situation can even be considered likely if, as appears to be the case in our experiments, the turbulent r.m.s. velocity is very much larger than the laminar burning velocity of the mixture. It goes without saying that such a flame structure destroys the validity of the theoretical formula, equation 9. In chapter 4, we will present experimental evidence regarding the mode of flame development which indicates that flame propagation is highly irregular.

c) Previous research into turbulent dust and gas explosions

Since it is difficult to achieve stationary, adiabatic dust flames for detailed observations, dust combustion has traditionnally been studied in constant volume bombs of various sizes and shapes, with emphasis being put of classifying dusts by such criteria as minimum explosible concentration, minimum auto-ignition temperature, etc., to allow for the design of safety measures appropriate for the safe handling of each dust. A number of people have attempted to measure the influence of turbulence by varying the delay between dispersion of the dust and ignition of the mixture. Turbulence associated with the dust dispersion process is not supported and hence must decay as the delay between dispersion and ignition is increased. This

type of experiments have been done by Moore[22,23], Bartknecht[24], Eckhoff[25], Cocks and Meyer[26], Swift[27] and Reeh[28]. These people found that the maximum pressure is affected very little by the ignition delay, but that the maximum rate of pressure rise decreases by a factor as high as 6, as the dispersion turbulence is allowed to decay. The rate of decay of the turbulence appeared to be closely connected with the minimum dimension of the combustion chamber, i.e. the maximum eddy size. This will be explored further in chapter 4, where we discuss the results of our own experiments with ignition delay variation. In a few of the abovementionned studies, the experiments were replicated with gas-air mixtures, i.e. the combustion chamber and dispersion bottle were filled with explosible gas-air mixture and the dispersion bottle was discharged, without any dust in the system at all. Here again, the maximum pressure, which in principle depends only on the energetics of the mixture, varied very little, but the K_g factor relaxed towards a laminar value as the ignition delay was increased. In the studies by Bartknecht and Moore, the ratio of the K factors of the dust and gas, K_{St}/K_g, was approximately constant over all the ignition delays studied, which indicates that the burning rate increase brought about by turbulence in dust is equal to that obtained in gas. In the experiments by Reeh, this pattern could not be so clearly observed.

Experiments in which the degree of turbulence was varied by adjusting the initial pressure of the dispersion bottle, while keeping the ignition delay constant, were performed by Nagy and Portman[29] with a coal-dust-air mixture and with a

hybrid mixture of coal-dust, methane and air in a 9.3 liter chamber. With the coal dust, the maximum rate of pressure rise increased linearly with dispersion pressure until a peak of 25,000 kPa/s was reached. Further dispersion pressure increases caused the K_{st} to drop. With the hybrid mixture, the maximum rate of pressure rise increased linearly over the whole range of dispersion pressures studied.

The influence of fan-generated turbulence on gaseous explosions in closed vessels has been studied by Harris[30] and more recently by Abdel-Gayed et al.[31] In Harris' study the maximum rate of pressure rise of pentane-air explosions in a 1.7 m^3 sphere increased linearly with fan speed. Measurements of pressure fluctuations in the turbulent premixture flow showed in turn that the turbulence intensity was directly proportional to the fan speed. This suggests the following simple correlation for the turbulent burning velocity:

(14)
$$\frac{S_t}{S_l} = 1 + k \frac{u'}{S_l}$$

Abdel-Gayed et al. measured burning velocity directly by the double kernel technique in a 22.2 liter cylindrical bomb fitted with four fans generating near-isotropic turbulence. For low turbulence intensities ($0 < u' < 2$ m/s) the burning velocity increased linearly with the turbulent r.m.s. velocity, in agreement with equation 14. For higher turbulence intensities the curves of S_t versus u' begin to flatten out, and with some mixtures, quenching of the flame was obtained with a sufficiently high value of u'. Because this extensive study has been performed with gas-air mixtures similar to ours,

and with state-of-the-art techniques of turbulence and burning velocity measurements, we will want to use its results to assess the features of the turbulent flow field in our own experiments.

Kauffman et al.[32] have recently studied turbulent dust explosions in a 1 m^3 spherical vessel in which the dust-air mixture was fed from six ports located symmetrically on the surface of the sphere. The turbulence intensity was adjusted by varying the air flow rate through the ports and, to a very good approximation, the turbulent r.m.s. velocity was directly proportional to the flow rate. The burning velocity of cornstarch-air mixtures, deduced from pressure measurements, was found to be directly proportional to the turbulent r.m.s. velocity.

III- EXPERIMENTAL CONSIDERATIONS AND PRELIMINARY EXPERIMENTS

a) Apparatus

A spherical vessel of 333 liter volume (figure 2), of 0.9 m diameter, and a cylindrical vessel of 180 liter volume, with 1 m height and 0.5 m diameter, were used in the present study to assess the influence of turbulence on dust and gas explosions in closed vessels.

In the spherical vessel, the dust was placed in a bowl at the bottom of the vessel and dispersion was achieved by an air blast from a 1.57 liter dispersion bottle discharging through a half-inch diameter tube nozzle directed at the center of the dust bowl. The dispersion was triggered by opening a solenoid valve in the dispersion circuit. Ignition was achieved by either an exploding fuse wire or a bare magnesium flashbulb filament located at the center of the vessel. The delay between dispersion and ignition could be controlled by means of an electric timer.

The features of the dispersion system provide us with two means of varying the intensity of the turbulence of the dust-air mixture at the moment of ignition. With a fixed initial pressure in the dispersion bottle, we can vary the delay between opening the dispersion solenoid valve and igniting the mixture; the longer the ignition delay, the more the flow field will have relaxed towards a quiescent state. Alternatively, with a fixed delay between dispersion and ignition, the dispersion bottle initial pressure can be varied; the higher the pressure, the bigger the swirl induced in the combustion chamber. Both these means of turbulence variation

were studied in the spherical bomb and the results are presented in chapter four.

The cylindrical vessel was fitted with accessories similar to those of the spherical one. Additionnal turbulence was generated in the cylindrical vessel by a 3.0 liter "turbulence bottle" which discharged through a port on the circumference of the vessel, near its center. The turbulence bottle was charged to the same pressure as the dispersion bottle and discharged simultaneously with it. Since it was desired to study explosions occurring at atmospheric initial pressure, it was necessary, in the cylindrical vessel experiments, to first evacuate the vessel to a level such that atmospheric pressure would just be recovered upon injection of gas by the turbulence and dispersion bottles. In the spherical vessel, this precaution was not taken because the mass injected by the dispersion bottle was a very small fraction of that initially present in the vessel. The results of experiments, performed in the cylindrical bomb, in which the pressure of the dispersion and turbulence bottles was varied, are presented in chapter 4.

It was desired to study the influence of jet-induced turbulence in conjunction with dispersion-induced turbulence in the spherical vessel. For this purpose, the vessel was fitted with two different turbulence-producing mechanisms and series of experiments were performed with each. One was a 45 cm diameter copper tubing ring (figure 4a) on which 16 holes of 1.1 mm diameter were drilled. The other was an 80 cm long vertical pipe (figure 4b), positioned 12 cm away from the vertical axis of the sphere, on which 12 holes of 9.5 mm diameter were drilled. The holes were arranged in four

stations, spaced 20 cm away from each other, each station comprising three holes spread at 120 degree intervals along the circumference of the tube.

The turbulence ring and turbulence pipe were fed by a high pressure (690 kPag) air supply and the level of turbulence generated by the jets could be controlled by varying the mass flow rate of air through the holes. In the case of the turbulence ring, the flow was choked at the orifices, so that the flow rate could be adjusted by varying the static pressure in the ring itself. In the case of the pipe, the hole area was too large to permit choking, hence the flow rate was modulated by a globe valve in the air supply circuit and measured from the time required to attain a certain pressure rise in the sphere.

The sequence of operations for dust explosion experiments with jet-induced turbulence was as follows. The dust was first weighed into the cup at the bottom of the vessel. The vessel was then put under a vacuum of 400 mm Hg. The air jets were turned on, and air addition from the jets caused the vessel pressure to increase again. When atmospheric pressure was restored, the dispersion air blast was activated and ignition followed after a predetermined delay. In the experiments done with methane-air mixtures, the vessel was first evacuated (to 600 mm Hg) and then filled by partial pressure with an amount of methane resulting in the desired composition. The air jets were then turned on, and the dispersion process was triggered when the vessel reached atmospheric pressure, followed by ignition. It is believed that the intense swirl generated by the jets was sufficient to mix the methane and air adequately.

A PCB quartz pressure transducer was used to record the pressure-time history in both the spherical and the cylindrical vessels; the maximum rate of pressure rise was calculated from the slope of a tangent to the pressure-time curve through its inflection point. An ion gauge was mounted on the surface of the spherical vessel, to monitor the time of flame arrival on the vessel wall. A typical oscilloscope record of a turbulent dust explosion is shown in figure 5.

b) Properties of the combustible mixtures

The dust used in the present study was cornstarch, a natural polymer of dextrose, with formula $(C_6H_{10}O_5)_n$. Peraldi[33] has measured its heat of combustion to be 631.5 kcal/mole and its heat of formation 222 kcal/mole. The literature seems to contain no information on the devolatilization properties (i.e. products, rate and enthalpy of devolatilization) of cornstarch. However, these properties should be very similar to those of cellulose, since these two compounds are identical in structure and vary only by the number of monomers making up a polymer chain. Devolatilization of thin strips (100 micron thickness) of cellulose fiber, with moderate heating rates and short residence time, has been studied by Lewellen et al.[34] who achieved complete devolatilization (i.e. no residual char) and found that the process could be described by the simple Arrhenius formula

$$\frac{dM}{dt} = -k \exp\left(\frac{-E_a}{RT}\right) M \qquad (15)$$

where M = mass of cellulose present in the sample

$k = 6.79 \times 10^{-9}\ s^{-1}$

E_a = 33.4 kcal/mole

R = universal gas constant

T = temperature

From the above formula, a characteristic time of devolatilization is determined to be

(16) $$\tau_{dev} = k^{-1} \exp\left(\frac{E_a}{RT}\right)$$

Table 1 shows how the time required for devolatilization varies as a function of temperature.

T, ^{o}K	τ_{dev}, sec
1000	2.2×10^{-3}
1200	1.4×10^{-4}
1400	1.9×10^{-5}
1500	8.8×10^{-6}
1600	4.4×10^{-6}
1800	1.4×10^{-6}
2000	5.6×10^{-7}

Table 1. Characteristic time of devolatilization as a function of temperature.

From this we can conclude that complete devolatilization of cornstarch occurs well before a temperature of about 1500 degrees K has been reached. Since the flame temperature of cornstarch-air mixtures (as calculated by the NASA code[35]) is of the order of 2000 degrees K, and since chemical reactions do not start occurring at a significant rate until the temperature reaches the vicinity of the flame temperature[36], it seems

likely that the burning will not start occurring before devolatilization is complete, i.e. burning will occur completely in the gas phase.

Commercially available starch usually contains about 10% moisture by weight. In the present study, the cornstarch was placed in an oven at 90 degrees C for about 18 hours prior to an experiment, to eliminate the moisture and thus help produce a more uniform dispersion. In a number of experiments, a fluidizing agent (CAB-O-SIL) was mixed with the cornstarch in the proportion of 0.5% of fluidizing agent per unit mass of mixture, to further improve the dispersion. A particle size analysis obtained via direct imaging with an optical image analyzer showed the average size of the particles to be 14.7 microns, with a standard deviation of 5.1 microns. Scanning electron micrographs (figure 6) showed the particles to be remarkably spheroidal in shape.

The laminar burning velocity of cornstarch-air mixtures has never been measured. Kauffman et al.[32] estimate the laminar burning velocity to be 0.40 m/s for a 300 gm/m^3 mixture and 0.70 m/s for a 700 gm/m^3 mixture, from extrapolation of their results of burning velocity versus turbulence intensity. This estimate, however, is highly sensitive to the method of determining the turbulent burning velocity and to the extrapolation scheme used to abstract the laminar burning velocity.

Marble [37] has shown that, from the thermodynamic point of view, a dust-air suspension, whose particles are so small that the velocity and temperature difference between the solid and gas phase is negligible, can be treated as a perfect gas whose

properties reflect a weighted average of the solid and gas phase. Since the characteristic velocity rise time of the particles in our suspension (i.e. the time required for any slip velocity to be reduced to 1/e times its original value as a result of Stokes drag), which can be shown to be

$$\tau_{vr} = \frac{2}{9} \frac{\rho_{dust} r_{dust}^2}{\mu} \tag{17}$$

and their characteristic temperature rise time (i.e. the time required for any temperature difference to be reduced to 1/e times its original value), which can be shown to be

$$\tau_{tr} = \frac{\rho_{dust} r_{dust}^2 c_p}{3 k_{air}} \tag{18}$$

are both of the order of milliseconds, i.e. a time span very short compared to the duration of an explosion, the assumptions of no slip and no temperature lag are valid, and the specific heat ratio of the dust-air mixture, which enters into the calculation of the burning velocity from pressure measurements (equation 9), can be taken as

$$\bar{\gamma} = \frac{c_{p\,air} + \kappa c_{dust}}{c_{v\,air} + \kappa c_{dust}} \tag{19}$$

where κ is the ratio of dust mass to gas mass per unit volume. For a 300 gm/m^3 mixture at 20 degrees C, we have

$$\bar{\gamma} = \frac{1.006 \frac{kJ}{kg\ ^oC} + \frac{300\ gm/m^3}{1209\ gm/m^3} \times 1.55 \frac{kJ}{kg\ ^oC}}{0.718 \frac{kJ}{kg\ ^oC} + \frac{300\ gm/m^3}{1209\ gm/m^3} \times 1.55 \frac{kJ}{kg\ ^oC}} \tag{20}$$

$$\overline{\gamma} = 1.26$$

Table 2 summarizes the properties of cornstarch that are relevant to its combustion characteristics.

Chemical formula:	$(C_6H_{10}O_5)_n$
Mol. wt. of monomer:	162
Density:	1.5 gm/cm^3
Stoichiometric concentration:	253.7 gm/m^3
Heat of combustion:	631.5 kcal/mole
Heat of formation:	222 kcal/mole
Specific heat:	0.37 kcal/kg-C

Table 2. Properties of cornstarch that are relevant to its combustion characteristics.

The methane used in the present study was of the commercially pure grade. The laminar burning velocity of a 7.5% methane-air mixture is reported by Andrews and Bradley[38] to be 0.28 m/s.

c) Preliminary experiments on the effects of dust concentration

To establish some confidence in the ability of the apparatus to produce repeatable and trustworthy results, the effect of varying dust concentration with a fixed ignition delay, fixed dispersion bottle pressure and without extra means of inducing turbulence was investigated. The dispersion bottle pressure was 1379 kPa and the ignition delay was set at 0.5 seconds after a few preliminary runs showed that this gave the highest value of P_{max} and $(dP/dt)_{max}$.

Figures 7 and 8 show maximum overpressure and K_{st} factor, respectively, as a function of cornstarch concentration for the 333 liter sphere and the 180 liter cylinder. For comparison purposes, results from Nagy[39], Hartmann[40] and Cocks and Meyer[26] are also shown. The peak overpressures are found to be in fair agreement with one another, in spite of the widely different properties of the cornstarch used and of the different characteristics of the experimental apparatuses. The K_{st} factor, on the other hand, is found to vary over a wider range. All the data for P_{max} show a similar trend, with P_{max} rising sharply from a lean limit concentration of about 100 gm/m^3 and asymptote to about 700 kPa when the concentration reaches 500 gm/m^3. No rich limit was observed up to a concentration of 1000 gm/m^3. The peak overpressure in the 333 liter sphere was consistently higher than that obtained in the 180 liter cylindrical vessel. This may be due to more severe heat losses to the walls in the cylindrical vessel since the flame is already in contact with the cylinder wall prior to complete consumption of the mixture at the ends of the vessel. For both vessels, the maximum pressure is far less than predicted from an equilibrium calculation[35] when the concentration is smaller than stoichiometric, but the theoretical and experimental curves seem to cross in the vicinity of 600 gm/m^3. The discrepancies could be caused by heat loss, settling or by the inability to predict pressure rise correctly from mere chemical equilibrium arguments.

The K_{st} from the cylindrical bomb show a maximum value of about 6000 kPa-m/s at a dust concentration of 200 gm/m^3 and then decreases with a further increase in concentration. The K_{st}

from the spherical vessel does not show the same trend: it simply increases asymptotically to a peak value of about 3500 kPa-m/s. Thus the burning rate in the cylindrical vessel, as indicated by the K_{st} factor, is generally higher than that from the spherical vessel.

IV- DISPERSION-INDUCED TURBULENCE

a) Influence of ignition delay

i- Influence of ignition delay on dust and gas explosions

Since the discharge of the dispersion bottle is a sudden, discrete event, the turbulence induced by the dispersion process will start to decay immediately after the dispersion bottle has been completely emptied and the fuel-air mixture will relax back towards a laminar state.

Figures 9 and 10 show the results of experiments in which the delay between dispersion and ignition was varied to try to elucidate the role played by the transient turbulence of the dispersion process. The experiments were done with a 450 gm/m^3 cornstarch-air mixture in the spherical vessel, with a 300 gm/m^3 cornstarch-air mixture in the cylindrical vessel and with a 7.5% methane-air mixture in the spherical vessel. The dispersion pressure used was 1379 kPa.

Figure 9 shows the maximum pressure developed, while figure 10 shows the ratio of K_{st} and K_g to the maximum K factor observed (this maximum value is given in the table below). This provides a convenient way of normalizing the data to compare the influence of the flow field on gas-air flames and dust-air flames.

Spherical bomb Methane-air	Spherical bomb Cornstarch-air	Cylindrical bomb Cornstarch-air
$(dP/dt)_{max}$:	$(dP/dt)_{max}$:	$(dP/dt)_{max}$:
16 456 kPa/s	6 895 kPa/s	4 496 kPa/s
K_g:	K_{st}:	K_{st}:
11 406 kPa-m/s	4765 kPa-m/s	2539 kPa-m/s

Table 3. Reference values for figure 10.

For both the cylindrical and the spherical vessels with dust and gas, the maximum overpressure and the maximum K factor are obtained with an ignition delay of approximately 0.5 seconds. Transient measurements of the dispersion bottle pressure show that this is just the time required for the bottle to become completely discharged. With shorter ignition delays, it appears that the dust and air have had insufficient time to mix homogeneously, while for longer delays, the turbulence of the dispersion has begun to die down and is less effective in enhancing flame propagation.

For both the 180 liter cylinder and the 333 liter sphere, the K_{st} factor measured with an ignition delay of 1.0 second is roughly 25% of the maximum K_{st} recorded.

Two causes can explain this sudden, violent decrease in the burning rate: settling of the dust particles, on the one hand, and decay of the dispersion-induced turbulence, on the other hand.

If we assume that the typical settling velocity of the dust particles is equal to their Stokes free fall velocity, then the characteristic settling time of the dust suspension, defined as the ratio of the average falling distance to the

settling velocity, is calculated to be

$$\tau_{set} = \frac{9\,\mu\,r}{2\,r_{dust}^2\,\rho_{dust}\,g} \tag{21}$$

where r is the sphere radius, in the case of the spherical vessel, or one half the cylinder height, in the case of the cylindrical vessel. Since this quantity is approximately equal to 50 seconds for single starch particles of 15 micron diameter, then it appears unlikely that significant settling can take place with ignition delays of the order of one second, if the suspension is made up of single particles. However, Bryant[41] has found that dust suspensions of the type studied here often consist of agglomerated particles whose settling time can be far less than that of single particles. Our experimental observation, that a 450 gm/m^3 starch-air mixture could not be ignited in the 333 liter sphere with an ignition delay of 1.0 second or longer (only one shot, with 1.5 second ignition delay, ignited and gave minimal pressure rise), seems to support this idea. In what concerns the shots that did ignite, however (ignition delay less than or equal to 0.9 seconds), the pressure deviation from the value observed with 0.5 seconds ignition delay was at most 30%, while the decrease in the maximum rate of pressure rise was by a factor of four. Referring back to figures 7 and 8, it seems unlikely that such a large decrease in the burning rate could result in such a relatively small decrease in the peak pressure, if it were caused primarily by a decrease in concentration.

We conclude that there is uncertainty as to whether settling or turbulence decay cause the observed variations. It

is probably true that both mechanisms affect combustion of the dust-air mixture, and that settling and turbulence decay are coupled processes.

It will be observed that in the 333 liter sphere, the ratio K/K_{max} falls far more steeply with time for the dust-air mixture than for the gas-air mixture. Although this could be due to settling of the dust particles, as discussed above, another cause can be cited. Dust remains in suspension in a gas by virtue of the viscous and pressure forces exerted by the gas on the suspended particles. In a turbulent dust-air suspension, therefore, energy is being dissipated not only by the shearing forces in the small-scale motions, but also by the work being done against the dust-suspending forces. Beer et al.[42] have estimated that the ratio of the kinetic energy dissipation rate in a dust-air mixture due to this effect (ε_p) to the dissipation rate that would be observed in the absence of dust particles (ε) was of the order of the mass fraction of dust present in the gas, i.e. $\varepsilon_p / \varepsilon \simeq \kappa$. In our particular case, the mass fraction is κ = (450 gm/m^3)/(1230 gm/m^3) = 37%. Hence the dissipation rate is significantly higher in the dust-air mixture than in the gas-air mixture.

ii- Characterization of the decay of the dispersion turbulence

In a closed vessel, decomposition of the fluid velocity into a mean and a fluctuating quantity is not possible since the closed boundaries do not allow the existence of a mean flow. Hence, in discussing the influence of "turbulence" on explosions in closed vessels, one has to be a little bit more

specific regarding what is meant by "turbulence" in this context.

The phenomenon of the decay of turbulence in a closed vessel has been studied experimentally by Tsuge et al.[43,44] who performed the following simple experiment. Tsuge et al. dragged a perforated plate, at a fixed speed, across a cylinder and measured the fluid speed, generated by the motion of the plate, at a hot-wire anemometer spaced 10 cm away from the wall of the cylinder (cylinder length: 60 cm), along its axis.

The flow pattern identified by Tsuge et al. consisted in large scale motions with a regular decay rate (Tsuge calls these motions "flow components"), on which were superimposed small, irregular, jagged motions whose amplitude decayed along with that of the flow components. The Fourier spectrum of these motions had a sharply peaked distribution, i.e. most of these motions corresponded to a fairly well-defined eddy size. Tsuge et al. made a parametric study of the factors which affected the decay rate of the flow components by varying the perforated plate hole spacing and diameter, the viscosity of the fluid, the piston speed and the diameter of the cylinder (diameters of 50, 100 and 150 mm were investigated). It was found that the method of generating the "turbulence", i.e. hole diameter and spacing, had very little influence on the decay rate, but that cylinder diameter was very important in controlling that rate. The best fit of the experimental data was obtained with

(22) $$Ge = k\, Re^{0.70}$$ where

(23) $$k = 1.73,$$

(24) $$Re \equiv \frac{uD}{\nu} ,$$

(25) $$Ge \equiv \left(\frac{\epsilon D^4}{\nu^3}\right)^{1/4} ,$$

(26) $$\epsilon \equiv \frac{u^2(t)}{2\,\theta(t)}$$

$\theta \equiv$ half-energy time, i.e. the time required for the kinetic energy, per unit mass of fluid, to be reduced by a factor of 1/2.

From equation 22, a relationship between u_0, the flow component speed at time zero, and u(t), the speed at any subsequent time, can be derived as follows:

(27) $$Ge = \left(\frac{u^2\, D^4}{2\,\theta\,\nu^3}\right)^{1/4} = k\left(\frac{uD}{\nu}\right)^{0.7}$$

(28) $$\frac{u^2 D^4}{2\,\theta\nu^3} = \frac{k^4 u^{2.8} D^{2.8}}{\nu^{0.8}}$$

(29) $$\theta\, u^{0.8} = \frac{D^{1.2}}{2\,k^4\nu^{0.2}} \equiv J$$

where J is a dummy variable used to regroup terms.

If we consider t to be a function of u, this gives

(30) $$t\,(u_i/2^{1/2}) - t\,(u_i) = J\,u_i^{-0.8}$$

Let us assume a relationship of the type

$$t = \alpha + \beta\, u_i^{-0.8} \tag{31}$$

where α and β are undetermined constants. Then

$$t\,(u_i/2^{1/2}) - t\,(u_i) = \left(\alpha + \frac{\beta\, u_i^{-0.8}}{\sqrt{2}^{-0.8}}\right) - \left(\alpha + \beta\, u_i^{-0.8}\right) = J\, u_i^{-0.8} \tag{32}$$

This is satisfied identically if

$$\beta = \frac{J}{\left(\frac{1}{\sqrt{2}^{-0.8}} - 1\right)} \text{ . Hence} \tag{33}$$

$$t = \alpha + \frac{J}{\left(\frac{1}{\sqrt{2}^{-0.8}} - 1\right)}\, u^{-0.8} \equiv \alpha + J'\, u_o^{-0.8} \tag{34}$$

At $t = 0$, $u = u_o$, so that $\alpha = -J'\, u_o^{-0.8}$:

$$t = J'\, u_o^{-0.8}\left[\left(\frac{u}{u_o}\right)^{-0.8} - 1\right] \tag{35}$$

$$\left(\frac{u}{u_o}\right)^{-0.8} = \left(\frac{t}{J'\, u_o^{-0.8}}\right) + 1 \tag{36}$$

$$\frac{u}{u_o} = \left[1 + \left(\frac{t}{J'\, u_o^{-0.8}}\right)\right]^{-1/0.8} \tag{37}$$

Absorbing the constants, with $\nu = 1.5 \times 10^{-5}$ m^2/s, this gives

$$u = u_o\left[1 + \left(\frac{0.6207\, u_o^{0.8}}{D^{1.2}}\right) t\right]^{-1.25} \tag{38}$$

Hence it seems that the quantity $t/D^{1.2}$ is the parameter governing the decay of the flow components. This can be interpreted to mean that the decay rate is governed by the size of the largest eddy in the vessel, i.e. the vessel diameter. If the dispersion turbulence decay in closed bombs follows the pattern identified in Tsuge's experiments, and if the "flow components" can be associated with a turbulence intensity, then there should be a relationship between the burning rate observed with a given ignition delay, and the amount by which the turbulence induced by the dispersion process has been allowed to decay. Since the ignition delay, τ_{do}, corresponding to the observation of the maximum K_{st}, also corresponds to the greatest intensity of turbulence, then closed vessel experiments should show a relationship between $K_{st}/K_{st\,max}$, the normalized burning rate, and $(\tau_d - \tau_{do})/D^{1.2}$, the normalized turbulence decay time.

In figures 11 and 12, we have attempted to see whether such a relationship existed. It is seen in figure 12 that all the data fall fairly well on a single curve, despite the wide variety of the vessel sizes and shapes and of the dust-air mixtures under study. The figure makes clear the simple relationships linking vessel size, turbulence decay and dust combustion rate.

In the methane-air explosions performed in the 333 liter spherical vessel, the characteristic decay time of the turbulence, which we define to be the interval over which the measured K factor decreases by 1/e times its original value, is seen to be (figure 10)

(39) $\tau_{de} = \tau_d\ (K_g = K_{g\ max}/e) - \tau_d\ (K_g = K_{g\ max}) = 2.0\ s - 0.6\ s = 1.4\ s$

Let us try to see whether this agrees with the prediction of the characteristic decay time from Tsuge's work. From equation 31, this predicted time is given by

(40) $$\frac{1}{e} = \frac{u}{u_o} = \left[1 + \left(\frac{0.6207\ u_o^{0.8}}{D^{1.2}}\right)\tau_{de}\right]^{-1.25}$$

(41) $$\tau_{de} = \frac{1}{0.6207}\left[\left(\frac{1}{e}\right)^{-4/5} - 1\right]\frac{D^{1.2}}{u_o^{0.8}}$$

(42) $$\tau_{de} = 1.97\ \frac{D^{1.2}}{u_o^{0.8}}$$

u_o, the turbulent velocity corresponding to the observation of $K_{g\ max}$, can be estimated by comparing the ratio S_t/S_l (or, equivalently, K_{gmax}/K_{gl}) obtained in our experiments with the results of Abdel-Gayed et al.[31] Since $K_{gmax}/K_{gl} = 16500/3100 = 5.3$, we have

(43) $$S_t = \left(\frac{S_t}{S_l}\right)S_l = 5.3 \times 0.28\ m/s = 1.5\ m/s$$

Abdel-Gayed et al. have shown that this is obtained in 8% methane-air with $u_o = 1.2$ m/s. Hence

(44) $$\tau_{de} = \frac{1.97 \times (0.9)^{1.2}}{1.2^{0.8}} = 1.50\ \text{seconds}$$

The experimentally observed turbulence decay rate, as measured by explosion burning rates, corresponds nearly exactly

to that predicted by Tsuge's results.

iii- Flame regularity

It was pointed out in chapter 2 that if flame propagation is regular, then in the case of a spherical vessel, the time of flame arrival on the vessel surface, the time at which the maximum rate of pressure rise is observed, and the time at which maximum pressure is reached, should all coincide. Yet our experiments with both dust and gas mixtures show that this is not the case. In general, the maximum rate of pressure rise occurs when the overpressure ratio $(P_f - P_i)/P_i$ is about half its final value, and the time of flame arrival on the vessel surface, as measured by an ionization probe on the wall, corresponds loosely to the time of maximum rate of pressure rise (figure 5).

In figure 13, we have plotted the ratio of time of flame arrival to the time at which 95% of the final pressure is attained, as a function of the ignition delay for 7.5% methane-air in the 333 liter sphere. As the ignition delay is increased and the burning relaxes towards a laminar state, the time of flame arrival approaches that of maximum pressure, indicating a more regular flame development.

For very turbulent flames, however, the development appears highly irregular. This behavior of dust explosion flames has also been noted by Kauffman et al.[32] It appears, then, that estimates of turbulent burning velocity based on pressure measurements can only be of limited validity.

b) Influence of dispersion pressure

i- Spherical bomb

With a fixed ignition delay, the intensity of the turbulence in a closed explosion vessel will be determined by how the features of the dispersion system are matched with those of the vessel. To be more specific, the intensity of the turbulence will be proportional to the dispersion bottle pressure and volume, since an increase in either of these two factors increases the "swirl" induced by the dispersion discharge, and will vary in inverse proportion to the vessel volume, since an increase in this increases the mass of fluid which must be swirled.

Figures 14 and 15 show the results of a series of experiments in which the dispersion bottle pressure was varied in the 333 liter sphere with a 300 gm/m^3 cornstarch-air mixture and a 7.5% methane-air mixture. The ignition delay in these experiments was set to be 0.5 seconds, as this has been previously shown to result in the least amount of decay. Figure 14 shows the maximum pressure developed as a function of pressure in the dispersion bottle. For the methane-air mixture there is very little variation in the maximum pressure developed: it is nearly constant at about 560 kPa , 18% below the theoretically calculated value of 684 kPa for adiabatic combustion.[35] For the starch-air mixture, there is a slight increase of P_{max} with dispersion bottle pressure: it goes from 475 kPa at 690 kPa dispersion pressure, to 655 kPa at 2069 kPa dispersion pressure. On the average, the observed maximum pressure is 587 kPa , 37% below the theoretically calculated value of 932 kPa for adiabatic combustion. The fact that the deviation from adiabatic behavior is more pronounced in the

case of dust than in that of gas is probably linked to the slower burning velocity of the dust-air mixture. Since flame development is irregular, the flame contacts the wall early in the flame travel and heat loss starts well before the maximum pressure has been reached - hence the total amount of heat loss depends on the time required for complete combustion, and since this time is larger for dust than it is for gas, the deviation from adiabatic pressure is also larger for dust than for gas.

It seemed appropriate to normalize the burning rates with respect to that observed in a "reference" laminar explosion of 7.5% methane-air. Hence in figure 15, we have plotted the ratio $K' \equiv K/K_{g\ lam}$, where $K_{g\ lam}$ is the K of a laminar gas-air explosion, versus pressure in the dispersion bottle. The value of $K_{g\ lam}$ was measured in the spherical bomb to be 2575.9 kPa-m/s. The formula of Bradley and Mitcheson [6] (equation 9) for spherical vessel explosion shows that this value corresponds to a laminar burning velocity of 33 cm/sec, in good agreement with the value of 28 cm/sec reported by Andrews and Bradley[38], especially if a correction is made to account for the burning velocity increase associated with adiabatic compression of the mixture. Both K_g' and K_{st}' increase monotonously with bottle pressure, although it seems that the increase begins to taper off when the dispersion pressure has reached about 1724 kPa. For a given intensity of turbulence, methane-air seems to burn much faster than cornstarch-air, the ratio K_g'/K_{st}' having a value of about four. The scatter in the values of K' is much more important than that observed in the maximum overpressures (figure 14). This is understandable, since P_{max} is primarily determined by the concentration of

fuel, whereas K' is highly sensitive to the random fluctuations in the turbulent flow field from one explosion to the next.

ii- Cylindrical bomb

Experiments similar to the ones described above were performed in the 180 liter cylindrical vessel. Here, turbulence of the dispersion bottle was supplemented by that of a 3.0 liter "turbulence bottle", charged at the same pressure as the dispersion bottle and discharging simultaneously with it through a port on the circumference of the vessel, near its center. A 300 gm/m^3 cornstarch-air mixture and a 7.5% methane-air mixture were investigated, with the ignition delay set at 0.5 seconds.

Figure 16 shows the maximum pressure developed as a function of bottle pressure, while figure 17 shows K', the normalized burning rate, versus bottle pressure. The results are qualitatively similar to those obtained with the spherical vessel. The maximum overpressure is affected very little by the bottle pressure, and the dust-air mixture deviates more from adiabatic behavior than does the gas-air mixture. Here again, a monotonous increase of K_g' and K_{st}' with increased bottle pressure is evident and K_g' is roughly 3 to 4 times larger than K_{st}' at a given bottle pressure. Thus the explosions behave in a manner similar to those performed with dispersion pressure variation in the spherical vessel, even though the structure of the turbulent flow induced by the two bottles in the cylindrical geometry must be different from that induced by the single bottle in the spherical geometry. On comparing figures 15 and 17, we see that the K' factor obtained at a given bottle

pressure, for both dust and gas, is roughly twice in the cylinder what it is in the sphere. The explanation could lie in the fact that a given bottle pressure induces a much bigger swirl in the cylinder than in the sphere, because the ratio of bottle volume (i.e. the volume responsible for the swirling) to combustion chamber volume (the volume being swirled) is higher in the cylinder: this ratio has a value of (1 l + 3 l)/180 l = 0.0222 for the cylinder and 1.57 l/333 l = 0.0047 for the sphere.

iii- Correlation of burning rate increases in different apparatuses

The burning rate increase due to the dispersion process in vessels with different sizes and dispersion systems can be quantitatively assessed by making a simple thermodynamic study of the parameters affecting the turbulent r.m.s. velocity induced by the dispersion.

Consider the following system:

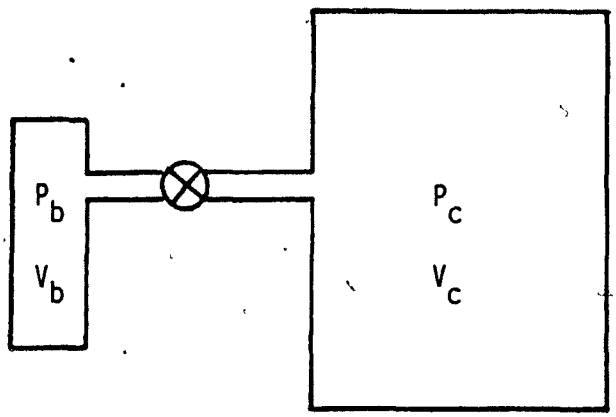

Let the subscripts
- i denote initial condition
- f denote final condition
- b denote the dispersion bottle

c denote the combustion chamber

We assume that the result of discharging the dispersion bottle is to impart a flow speed u' to the whole gas, without viscous dissipation taking place before the discharge if complete. Conservation of energy then requires

$$(45) \qquad U_{bi} + U_{ci} = U_{bf} + U_{cf} + \frac{1}{2}(m_{bi} + m_{ci})\, u'^2$$

With $U = m\, c_v\, T$ and $PV = mRT$, this gives

$$(46) \quad P_{bi}V_b c_v + P_{ci}V_c c_v = P_{bf}V_b c_v + P_{cf}V_c c_v + \frac{1}{2}\frac{(P_{bi}V_b + P_{ci}V_c)}{T_i}\, u'^2$$

$$(47) \qquad u'^2 = 2\, c_v T_i \left[\frac{V_b\,(P_{bi} - P_{bf}) + V_c\,(P_{ci} - P_{cf})}{P_{bi}V_b + P_{ci}V_c}\right]$$

$$(48) \qquad u'^2 = 2\, c_v T_i \left[1 - \left(\frac{P_{bf}V_b + P_{cf}V_c}{P_{bi}V_b + P_{ci}V_c}\right)\right]$$

If the dispersion bottle volume is small compared to the vessel volume, then the initial and final chamber pressures will be nearly equal. Since the flow stops when the bottle pressure equals the vessel pressure, this gives

$$(49) \qquad P_{cf} \simeq P_{ci} = P_{bf} \equiv P_c$$

Hence

$$(50) \qquad u'^2 = 2\, c_v T_i \left[1 - \left(\frac{P_c\,(V_b + V_c)}{(P_{bi} - P_c)\,V_b + P_c\,(V_b + V_c)} \right) \right]$$

$$(51) \qquad u'^2 = 2\, c_v T_i \left[1 - \left(1 + \frac{(P_{bi} - P_c)\,V_b}{P_c V_c} \right)^{-1} \right]$$

With the assumptions that $P_{bi} \gg P_c$, $V_c \gg V_b$, this gives

$$(52) \qquad u'^2 = 2\, c_v T_i \left[1 - \left(1 - \frac{P_{bi} V_b}{P_c V_c} \cdots \right) \right]$$

In first approximation, then, u' and $(P_{bi}V_b/P_cV_c)^{\frac{1}{2}}$ vary in direct proportion with each other. If the burning rate is linked to the turbulence intensity in a simple manner, such as

$$(53) \qquad \frac{S_t}{S_l} = 1 + k\, u' \; --$$

then results of closed vessel experiments in which the explosion of a gas-air mixture is accelerated by dispersion-induced turbulence should show the pattern

$$(54) \qquad \frac{K_{gmax}}{K_{glam}} = 1 + k(P_{bi}V_b/P_cV_c)^{1/2}$$

In figure 18, we have plotted the ratio K_{gmax}/K_{glam} versus $(P_{bi}V_b/P_cV_c)^{\frac{1}{2}}$ obtained by different researchers with

bombs of various sizes and shapes and dispersion systems with different pressures and volumes. Since some researchers did not perform truly laminar explosions in their experiments, we approximated K_{glam} to be the K factor obtained with an ignition delay equal to five times the ignition delay corresponding to the observation of the maximum K factor. The observation of K_{gmax} corresponds to the smallest possible amount of viscous dissipation in the particular apparatus, and thus corresponds most closely to the conditions of analysis described above. A linear increase of K_{gmax}/K_{glam} with $(P_{bi}V_b/P_cV_c)^{\frac{1}{2}}$ is observed. Thus the burning rate increase due to the turbulence of the dispersion process is simply related to the size and pressure of the dispersion bottle and of the combustion chamber.

V- JET-INDUCED TURBULENCE

It has been seen that the turbulence associated with the dispersion process has a transient, decaying nature. In experiments in which the delay between dispersion and ignition was varied, it was difficult to decouple the effects of dust settling on the one hand, and of turbulence decay on the other hand. Hence it was thought worthwhile to study the effect of a turbulent flow which would not have any direct impact on the dust-air suspension.

A convenient means of achieving this is by blowing air from a series of jets into the combustion chamber. For this purpose, two different devices were constructed and installed in the 333 liter spherical vessel: we shall designate them by the names of "turbulence ring" and "turbulence pipe". The turbulence ring was installed vertically in the center of the vessel. Because eight of the sixteen holes on the ring were drilled on one side of the copper tube, while the other eight were on the opposite side, the flow of air through the ring induced a tangential swirl in the combustion chamber. Hence it is sensible to think that only a small portion of the kinetic evergy flux $1/2\ \dot{m}\ c^2$ into the sphere went into "turbulent" random velocity fluctuations. The rest was going to support the swirling motions which, since they were perpendicular to the direction of flame propagation, did not directly contribute to acceleration of the flame. The dispersion bottle pressure used in experiments done with the turbulence ring was 1034 kPa and the ignition delay was 0.5 seconds; total ring flow rates varying from 0 to 14.9 g/s were investigated.

The purpose of constructing the turbulence pipe was to investigate higher turbulence intensities than had been achieved with the turbulence ring. The total hole surface in the turbulence pipe was 6.25 times greater than that in the turbulence ring - this allowed us to achieve total flow rates as high as 38.7 g/s with the same air supply system. In the turbulence pipe, the holes were drilled at 120 degree intervals on the surface of the copper tube: this geometry does not induce a tangential swirl and it is thought that the turbulence pipe is a more effective means of inducing turbulence than the turbulence ring. In experiments done with the turbulence pipe, the dispersion bottle pressure was increased to 2069 kPag, in an attempt to further increase turbulence intensity. The ignition delay was kept at 0.5 seconds.

Kauffman et al.[32] have measured that the turbulent r.m.s. velocity induced by blowing jets through six ports located symmetrically on the circumference of a 1 m^3 sphere was, to a very good approximation, directly proportional to the total jet flow rate. Hence a similar dependence can be expected in this study.

a) Dispersion-induced turbulence and jet-induced turbulence

Before comparing the influence of jet-induced turbulence on dust-air and gas-air explosions, it was thought instructive to acquire a feel for the relative importance of the dispersion-induced turbulence and the jet-induced turbulence in the 333 liter sphere. For this purpose, the following experiment was devised: the influence of ring jet flow rate on the maximum rate of pressure rise was studied with a 7.5%

methane-air mixture. In one case, the dispersion bottle was not used: turbulence was due to the ring jets alone. In the other case, the dispersion bottle was charged with methane-air mixture up to a pressure of 1034 kPa, hence the burning rate increase was due both to ring and jet turbulence. The results of the experiments are shown in figures 19 and 20. For both series of shots, the observed maximum rate of pressure rise, and therefore the turbulent burning velocity, increases linearly with jet mass flow rate. For such low turbulent burning velocities, Abdel-Gayed et al. have found a linear dependence of S_t on u'. Hence it appears that, both with and without dispersion, the turbulent r.m.s. velocity induced by the jets is directly proportional to the jet flow rate - a result similar to that obtained by Kauffman et al. The maximum rate of pressure rise, for a given ring flow rate, was consistently higher with the dispersion than without - clearly indicating the additional role played by the dispersion in enhancing the burning rate. The discrepancy between the two sets of results diminishes as we go to higher and higher flow rates, indicating that at high flow rates, the influence of the dispersion has faded and the flow field is dominated by the influence of the ring jets.

It is seen that the maximum pressure is significantly higher in the experiments without dispersion-induced turbulence than in those with it. This may at first appear paradoxical, since the faster burning in the experiments with the dispersion should reduce heat losses, and since the extra mass of mixture in the dispersion bottle should yield an additional pressure of

$$(55) \quad \Delta P_f = \frac{P_f}{P_i} \Delta P_i = \frac{P_f}{P_i} P_d \frac{V_d}{V_c} \simeq \frac{785}{101} \times 1135 \text{ kPa} \times \frac{1.57}{333} = 41.6 \text{ kPa}$$

However, a close examination of the experimental records indicates that flame development is much more regular in experiments without dispersion-induced turbulence than in those with it. As seen in figures 21a and 21b, the flame arrives on the vessel wall just before combustion is complete when the dispersion is not used, whereas it arrives much earlier when it is used. The greater time of flame contact with the walls, in the experiments with dispersion turbulence, results in greater heat losses which explain the measured discrepancies of peak pressure. The simplest explanation is that the tangential swirl of the ring jets alone promotes regular, orderly flame development, whereas the random, irregular motions from the dispersion tend to destroy it.

b) Influence of ring-jet flow rate

We performed a series of experiments with 300 gm/m^3 cornstarch-air and 7.5% methane-air, in which the turbulence of the dispersion process was supplemented by that generated by air jets blowing into the combustion chamber from the turbulence ring. This has the effect of altering both the intensity and the detailed structure of the fluid motions. The results for maximum overpressure and rate of pressure rise as a function of mass flow rate through the ring are presented in figures 22 and 23 respectively.

Both for dust and methane, the maximum overpressure remains remarkably constant with mass flow rate. This firmly

establishes the fact that the mass of dust consumed in an explosion is insensitive to the ring jet flow rate and that the effects of jet flow rate on the maximum rate of pressure rise, displayed in figure 23, are not caused by changes in the effective dust concentration, but rather by turbulence itself. In figure 23, K_g' and K_{st}' increase monotonously, K_g' is typically 3 to 4 times higher than K_{st}' and the relative increase in burning rate due to increased mass flow rate, which we define as $\Delta K'/K'\Delta\dot{m}$, is about the same for the dust-air as for the gas-air. These results parallel the situations observed with dispersion pressure variation in the sphere (figure 15) and bottle pressure variation in the cylinder (figure 17). The scatter observed in the values of K' is much higher for dust-air than for methane-air, perhaps owing to the difficulty in achieving a consistently homogeneous mixture of dust and air with the kind of dispersion system used in this study.

c) Influence of pipe jet flow rate

The experiments done with the turbulence ring were repeated with the vertical turbulence pipe, with the objective of investigating the effect of modifying the geometry of the jets and of studying a range of turbulence intensities higher than those which could be achieved with the turbulence ring. For this specific purpose, the turbulence pipe was designed to handle total air flow rates as high as 40 gm/s and the experiments were performed with a dispersion pressure of 2069 kPag. The results for maximum overpressure and K' as a function of mass flow rate are presented in figures 24 and 25 respectively.

The results are qualitatively similar to those obtained with the turbulence ring. The maximum overpressure of methane-air deviates very little from an average of 635 kPa. This is somewhat higher than the average value from previous experiments, probably owing to the additionnal mass of mixture associated with the high bottle pressure.

In this case again, K_g' and K_{st}' increase monotonously with turbulence intensity, K_g' is typically 3 to 4 times higher than K_{st}' and the relative increase in burning rate due to increased mass flow rate, $\Delta K'/K'\Delta\dot{m}$, is about the same for the dust-air mixture as for the gas-air. There was no evidence of turbulent quenching either for dust-air or methane-air, even for the highest K' (K_g'=10.8, K_{st}'=3.77) observed at a mass flow rate of 38.7 g/s.

VI - SUMMARY AND CONCLUSION

a) Synthesis of the experimental results

The experimental results presented in chapters four and five show that, for a substantial variety of turbulent flow structures and turbulence intensities, the relative burning rate variations caused by variation of the turbulence intensity are equal in a cornstarch-air mixture and a methane-air mixture. This result has been obtained with all methods of turbulence generation studied with the exception of ignition delay variation, where we have seen that the discrepancies between dust and gas behavior could be explained in terms of the settling of the dust particles or of the faster decay of turbulence in a dust-air mixture because of the work being done against the dust-suspending forces.

The finding that dust and gas respond to turbulence in a similar manner suggests that we use K_g' as a scale against which to compare K_{st}'. In figure 26, we have attempted to present a unified picture of the experimental results by plotting the relationship between the quantities K_g' and K_{st}' obtained under identical conditions of turbulence in each of the following four experimental set-ups: dispersion pressure variation in the sphere, bottle pressure variation in the cylinder, ring and pipe mass flow rate variation in the sphere. It is seen that K_g' and K_{st}' vary in linear proportion with each other, the data being best represented by the formula

$$K'_{st} = 0.30\ K'_g \qquad (56)$$

This suggests that the ratio of the burning rates of the dust-air mixture and the gas-air mixture is not sensitive to differences in the detailed structure of the turbulence induced by the various devices used, but that it rather depends on the physico-chemical properties of the mixtures themselves. Although we would need to know more about the fundamental characteristics of the cornstarch-air mixture (in particular, its laminar burning velocity and its laminar flame thickness) to draw a more definite conclusion from the results shown in figure 26, two possible explanations can be put forward at this time.

The first hypothesis is that the laminar burning velocity of the cornstarch-air mixture is about 0.30 times smaller than that of the methane-air and that the physical mechanisms responsible for the burning rate increase are the same in the two mixtures. Since it is known that, for the relatively small intensities of turbulence studied in this investigation, the main effect of turbulence on gas-air flames is to wrinkle the flame front so as to increase the total burning area, this hypothesis would imply that the dust-air flame and the gas-air flame are being wrinkled in the same proportion, so that the ratio of their turbulent velocities ($S_{st}/S_g = K_{st}'/K_g' = 0.30$) would simply be equal to the ratio of their laminar burning velocities. This "wrinkled laminar flame" regime of turbulent dust flame propagation would require that the thickness of the laminar dust-air flame be smaller than the smallest characteristic length scale of the velocity fluctuations.[16]

The second hypothesis is that, while the laminar burning velocities of the two mixtures may be close to one another, the

laminar dust-air flame is much thicker than the gas-air flame, and consequently, the modes of action of turbulence are different in the two media. If the laminar dust-air flame is thicker than the smallest length scale of the velocity fluctuations, its area can only be minimally affected by these fluctuations, and the more significant effect of turbulence will be to increase the rate of the transport processes taking place within the flame itself. This might be a less efficient mechanism of burning rate increase than flame wrinkling, and this could explain the observed discrepancies in the combustion rates of cornstarch-air and methane-air.

The approach used in this study has been to relate the maximum rate of pressure rise observed in an explosion to a parameter characterizing the intensity of the turbulence in the explosion (e.g. ignition delay, dispersion pressure, etc.) In order to make our results comparable with those of other workers, however, we need to express them in terms of more fundamental quantities: the burning rate should be expressed as a turbulent burning velocity and the turbulence should be described either by its r.m.s. velocity or by a quantity, such as the turbulent Reynolds number, representing both its intensity and its characteristic length scale.

A fair estimate of the turbulent burning velocity at the moment of maximum rate of pressure rise can be obtained through the use of the formula of Bradley and Mitcheson[6], equation 9. Since Abdel-Gayed et al.[31] have measured the turbulent burning velocity in a 22.2 liter cylindrical vessel where isotropic turbulence was being generated by four fans, it is possible to infer the turbulent r.m.s. velocity in our apparatus by

comparing our ratio of turbulent to laminar burning velocity of methane-air in a particular situation to the results of Abdel-Gayed et al. This allows us to show, in figure 27, the burning velocity as a function of turbulent r.m.s. velocity. The results are presented for jet-induced turbulence only, since it is obvious that experiments with jet-induced turbulence would show the same trend.

Although it is admitted that this method of data reduction has definite shortcomings (the correlation of S_t and u' obtained for methane by Abdel-Gayed et al. may not be applicable to our apparatuses where the structure of the turbulent flow is different; the Bradley-Mitcheson formula assumes spherical, regular flame development which is known not to be obtained in practice, to name but two), it is still thought to be of some use to obtain a rough estimate of the dependence of burning velocity on turbulent r.m.s. velocity. The relationship between S_t and u' for the dust-air mixture appears linear, although the scatter in the data is too large to notice a definite trend. It is unsafe to extrapolate from our results a value for the laminar burning velocity of 300 gm/m^3 cornstarch-air, although it appears that this value cannot be higher than about 30 cm/s.

b) General conclusions

From the results of our experiments, we are now in a position to draw a few definite conclusions regarding the validity of the approach we took to attack the problem and regarding the nature of the problem itself.

Although the crudeness of the method of dispersing dust used in our experiments creates uncertainties as to the homogeneity of the mixture and the constancy of the total amount of dust in suspension, the fact that maximum overpressures remained practically constant as we varied the intensity of the turbulence, while the maximum rates of pressure rise varied by a factor as high as eight, is proof that the extent of the reaction in our experiments was insensitive to whatever inhomogeneities may have been present and that the observed burning rate variations were associated with turbulence itself. We conclude that the crude experimental set-ups we used to study turbulent dust explosions are adequate for their intended purpose and that efforts to improve the means of suspending the dust by the use of more sophisticated devices can only be of marginal usefulness.

We have established that the relative burning rate increases brought about by turbulence in dust-air explosions are equal to those observed in gas-air explosions performed under identical conditions of turbulent flow. This result is not obvious a priori, since the structure and propagation mechanisms of turbulent flames are expected to differ widely in the two media. Although the proper physical interpretation of this result woud require further studies, it is felt that the result itself demonstrates the usefulness of studying gas-air explosions in conjunction with dust-air explosions. Since the turbulent flow field ahead of a turbulent explosion flame is constantly evolving, and since, in any case, a precise definition of turbulence in the context of a closed vessel without mean flow is difficult, it is felt that it is more

meaningful to relate the burning rate of a dust-air explosion to that of a gas-air explosion taking place under identical conditions, than to relate it to some characteristic value of the velocity fluctuations in the unburned mixture prior to ignition.

c) Recommendations for future work

The interesting results obtained in the course of this study have raised more questions than they have answered. While a strong correlation has been observed between the effects of turbulence on dust-air and gas-air explosions in closed vessels, the central questions of the structure and propagation mechanisms of a dust-air flame remain unanswered. It appears, however, that the use of gas explosion as a probe to study dust explosion can help speed up the learning process for the elucidation of these important issues.

A knowledge of the fundamental characteristics of laminar dust-air flames is required before the effects of turbulence on dust explosions displayed in this study can be properly interpreted. It is suggested that flat flame burner studies, concentrating on measurement of the laminar flame thickness and the laminar burning velocity, and evaluation of the modes of energy transport of cornstarch-air flames, could help clarify the relationship between the relevant length and velocity scales of dust-air flames and gas-air flames, and therefore constitute the next logical step in this area of research. While the difficulties of generating a uniform, stable dust-air suspension have plagued this type of studies in the past, it now appears that the fluidized bed techniques developed by

Veyssiere [45] and Peraldi [33] can help overcome these problems and lead to rapid progress in this field.

ii- REFERENCES

1- Corey, R.C. Chemical Engineering, 16 January 1978, pp. 111-119.

2- Sliz, J. First National School on Explosibility of Industrial Dusts. Karpacz, Poland, 1978, pp. 119-126.

3- Kauffman, C.W. Proc. International Meeting on Fuel-Air Explosions, SM Study 16, Eds. C.M. Guirao and J.H. Lee, University of Waterloo Press, Waterloo, 1982.

4- Tipler, W. Power Plants and Future Fuels. Institution of Mechanical Engineers, London, 1976.

5- Andrews, G.E., Bradley, D. and Lwakabamba, S.B. Combustion and Flame, 24, 285-304 (1975).

6- Bradley, D. and Mitcheson, A. Combustion and Flame, 26, 201-217 (1976).

7- Tennekes, H. and Lumley, J.P. A First Course in Turbulence. MIT Press,Cambridge, Massachusetts, 1972.

8- Tennekes, H. Physics of Fluids, 11, 669-670 (1968).

9- Tabaczynski, R.J., Ferguson, C.R. and Radhakrishnan,K. SAE Paper no. 770647, 1977.

10- Hires, S.D., Tabaczynski, R.J. and Novak, J.H. SAE Paper no. 780232, 1978.

11- Tabaczynski, R.J., Trinker, F.H. and Shannon, B.A. Ford Motor Company, 1978.

12- Ohta, Y. Proceedings of Workshop on the Gas Flame Structure, Novosibirsk, U.S.S.R., 1984.

13- Chomiak, J. Prog. Energy Combust. Sci., 5, 207-221 (1979).

14- Damkohler, G. Zeitschrift Electrochemie Angewandte Phys. Chem., 46, 601 (1940). (English translation NACA TM 1112 (1947))

15- Abdel-Gayed, R.G. and Bradley, D. Phil. Trans. Roy. Soc. London, 301, A1457, 1981.

16- Williams, F.A. Combustion and Flame, 26, 269-270 (1976).

17- Gaydon, A.G. and Wolfhard, H.G. Flames - Their Structure, Radiation and Temperature. Chapman and Hall, London, 1960.

18- Smoot, L.D. Private communication.

19- Mason, W.E. and Wilson, M.J.G. Combustion and Flame, 11, 195-200 (1967).

20- Bartknecht, W. Explosions - Course - Prevention - Protection. Springer Verlag, New York, 1980.

21- Karlovitz, B. 4th Symposium (International) on Combustion, Cambridge, Massachusetts, 1952.

22- Moore, P.E. Chemistry and Industry, p. 430, 1979.

23- Moore, P.E. I. Chem. E. Symposium Series no. 58, Rugby, 1980.

24- Bartknecht, W. Staub Reinhaltung der Luft, 31, 28 (1971).

25- Eckhoff, R.K. First International Colloquium on the Explosibility of Industrial Dusts. Baranow, Poland, 1984.

26- Cocks, R.E. and Meyer, R.C. Fabrication and Use of a 20 liter Spherical Dust Testing Apparatus. Process Specialties Section, Engineering Division, Procter and Gamble, Cincinnati, Ohio.

27- Swift, I. Proc. International Meeting on Fuel-Air Explosions, SM Study 16, Eds. C.M. Guirao and J.H. Lee, University of Waterloo Press, Waterloo, 1982.

28- Reeh, D. Staub Reinhaltung der Luft, 31, 12-21 (1971).

29- Nagy, J. and Portman, W.M. U.S. Bureau of Mines R.I. 5815, 1961.

30- Harris, G.F.P. Combustion and Flame, 11, 17-25 (1967).

31- Abdel-Gayed, R.G., Al-Khishali, K.J. and Bradley, D. Proc. Roy. Soc. London, A391, 393-414 (1984).

32- Kauffman, C.W., Srinath, S.R., Tezok, F.I., Nicholls, J.A. and Sichel, M. 20th Symposium (International) on Combustion, Ann Arbor, Michigan, 1984.

33- Peraldi, O. These de Docteur Ingenieur, Universite de Poitiers, 1985.

34- Lewellen, P.C., Peters, W.A. and Howard, J.B. 16th Symposium (International) on Combustion, Cambridge, Massachusetts, 1976.

35- Gordon, S. and McBride, B.J. Computer Program for Calculation of Complex Chemical Equilibrium Compositions, Rocket Performance, Incident and Reflected Shocks, and Chapman-Jouguet Detonations. National Aeronautics and Space Administration, Washington, 1971.

36- Lee, J.H.S. Phenomenology of Gas Explosions. McGill University, Montreal, 1980.

37- Marble, F.E. Proc. 5th AGARD Colloq. Combust. Propul., Braunschweig, pp. 175-213, 1962.

38- Andrews, G.E. and Bradley, D. Combustion and Flame, 19, 275-288 (1972).

39- Nagy, J., Seiler, E.C., Conn, J.W. and Verakis, H.C. U.S. Bureau of Mines R.I. 7507, 1971.

40- Hartmann, I., Cooper, A.R. and Jacobson, M. U.S. Bureau of Mines R.I. 4725, 1951.

41- Bryant, J.T. Combustion and Flame, 20, 138-139 (1973).

42- Beer, J.M., Chomiak, J. and Smoot, L.D. Prog. Energy Combust. Sci., 10, 177-208 (1984).

43- Tsuge, M., Kido, H. and Yanagihara, H. Bulletin of the J.S.M.E., 16, 244-251 (1973).

44- Tsuge, M., Kido, H., Kato, K. and Nomiyama, Y. Bulletin of the J.S.M.E., 17, 587-594 (1974).

45- Veyssiere, B. These de Docteur Ingenieur, Universite de Poitiers, 1978.

iii- LIST OF FIGURES

19- Effect of ring jet flow rate on P_{max} in 7.5% methane-air explosions in the 333 liter spherical vessel

20- Effect of ring jet flow rate on maximum rate of pressure rise in 7.5% methane-air explosions in the 333 liter spherical vessel

21a- Scope record of 7.5% methane-air explosion with ring jets, without dispersion blast

21b- Scope record of 7.5% methane-air explosion with ring jets, with dispersion blast

22- Effect of ring jet flow rate on P_{max} in the 333 liter spherical vessel

23- Effect of ring jet flow rate on maximum burning rates in the 333 liter spherical vessel

24- Effect of pipe jet flow rate on P_{max} in the 333 liter spherical vessel

25- Effect of pipe jet flow rate on the maximum burning rates in the 333 liter spherical vessel

26- Relationship between dust burning rate and methane burning rate in identical turbulent flow situations

27- Variation of turbulent burning velocity with turbulent r.m.s. velocity, for starch and methane explosion in the 333 liter spherical vessel with jet-induced turbulence

iv- FIGURES

FIGURE 1 - LENGTH SCALES INVOLVED IN TURBULENT DUST FLAME PROPAGATION

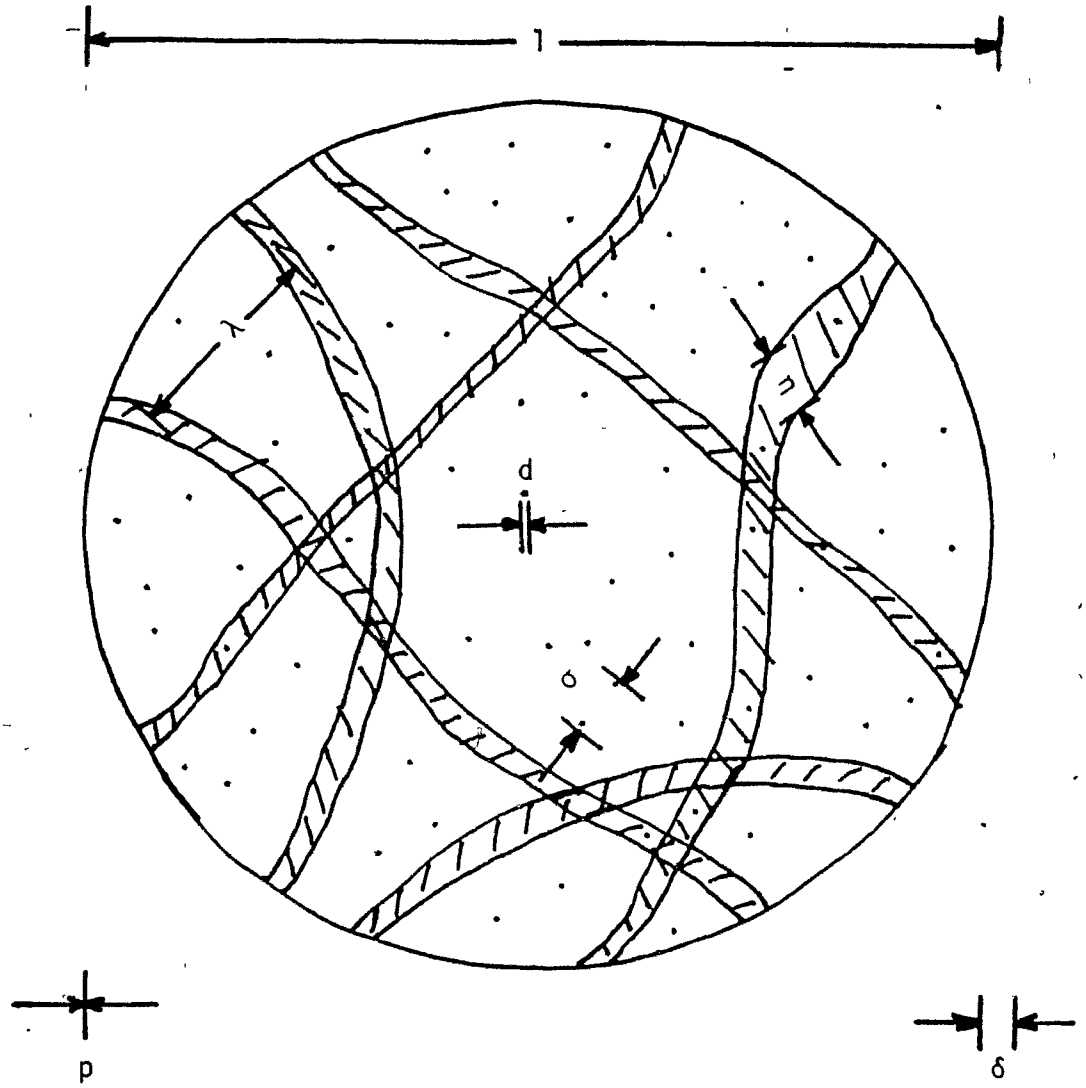

LENGTH SCALE	SYMBOL	ORDER OF MAGNITUDE
INTEGRAL LENGTH SCALE	l	10^{-2} m
TAYLOR MICROSCALE	λ	10^{-3} m
KOLMOGOROFF SCALE	η	10^{-4} m
PARTICLE SIZE	d	1.5×10^{-5} m
INTER-PARTICLE SPACING	σ	1.5×10^{-4} m
THICKNESS OF LAMINAR GAS FLAME	δ	10^{-4} m
MOLECULAR MEAN FREE PATH	p	10^{-8} m

TEST APPARATUS
(V = 0,333 m³)

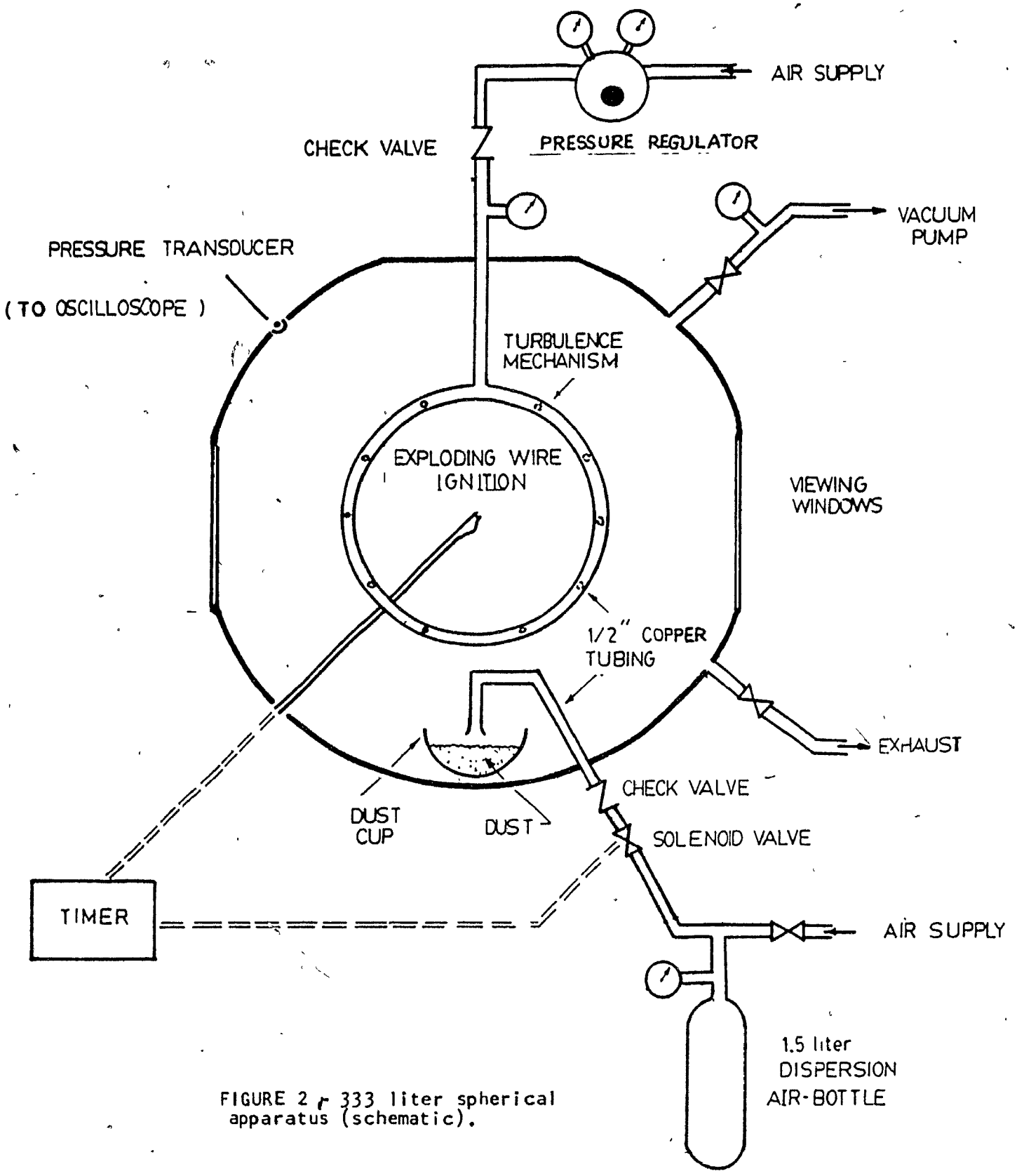

FIGURE 2 - 333 liter spherical apparatus (schematic).

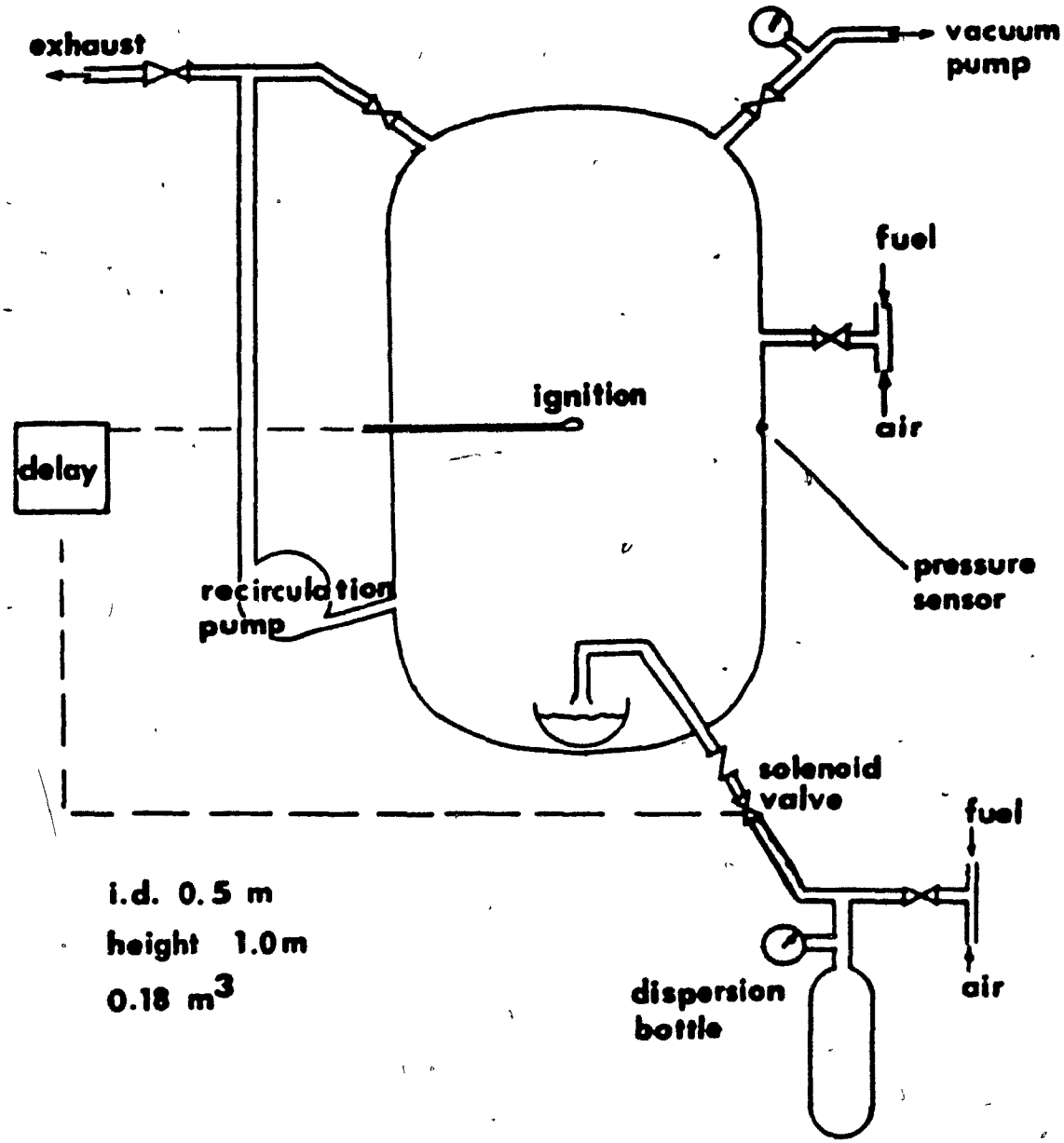

FIGURE 3 - 180-liter cylindrical vessel

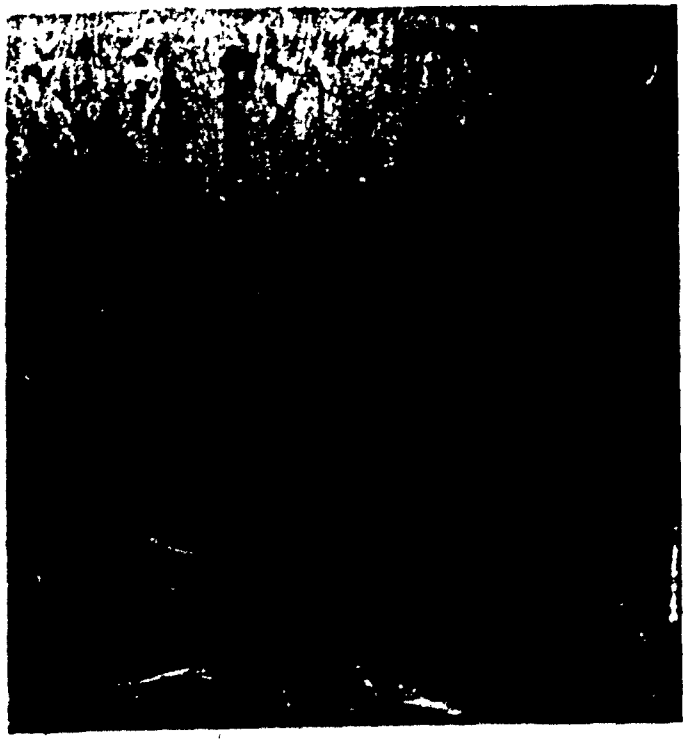

FIGURE 4a - Turbulence ring

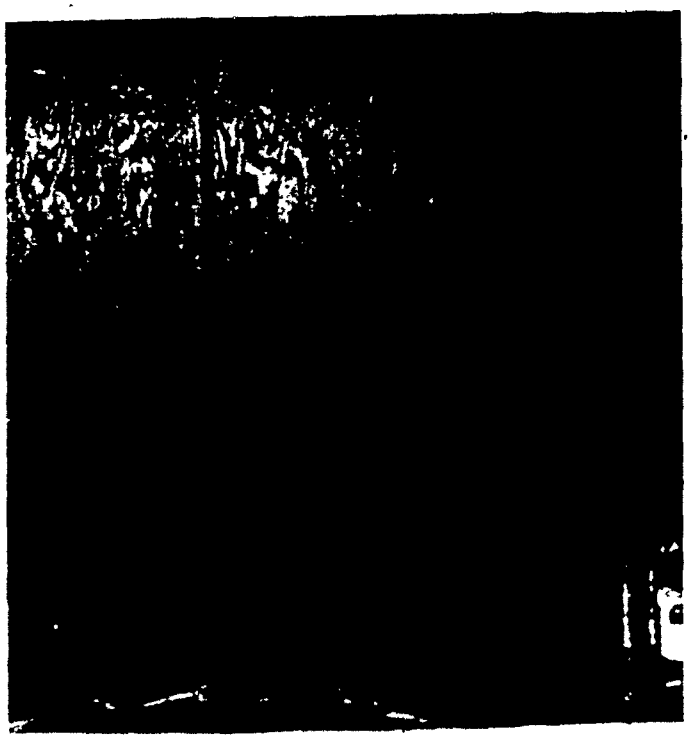

FIGURE 4b - Turbulence pipe

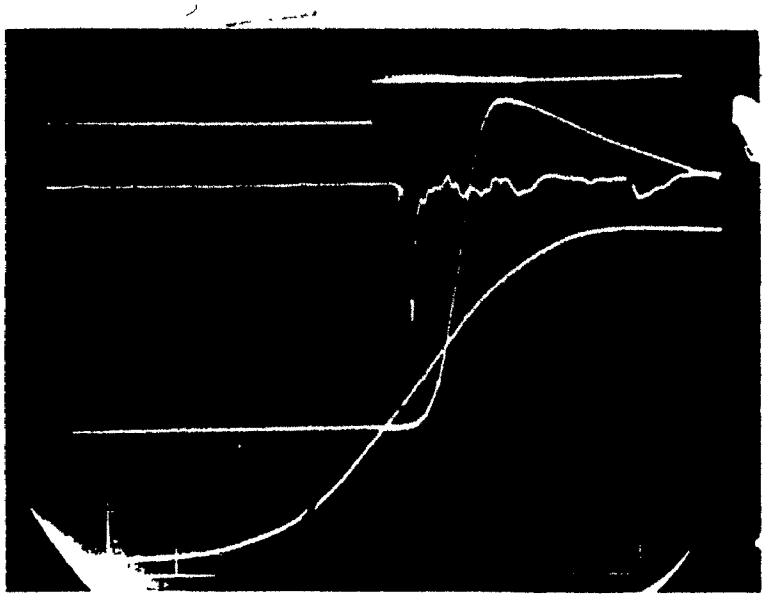

FIGURE 5 - Scope record of a dust explosion. The first and third trace (starting from the top) are triggered upon dispersion and sweep at 0.1 second per division. The second and fourth trace are triggered 0.5 seconds after dispersion and sweep at 0.01 second per division. Trace 1 is a witness trace showing the moment of ignition. Trace 2 is the ion probe record. Traces 3 and 4 show pressure, at 100 kPa per vertical scope division.

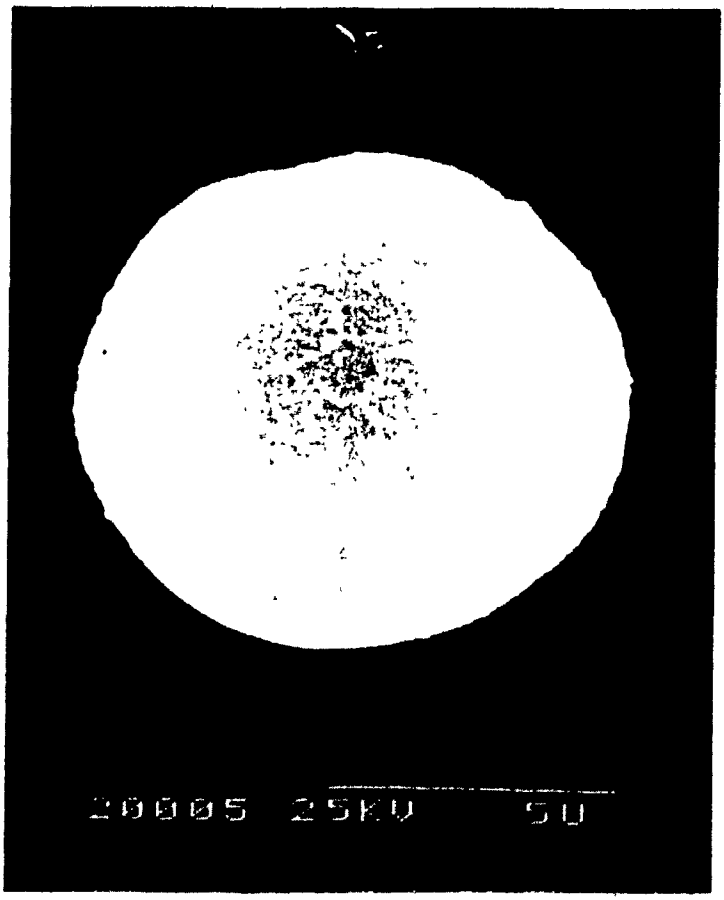

FIGURE 6 - S.E.M. photograph of cornstarch particle.

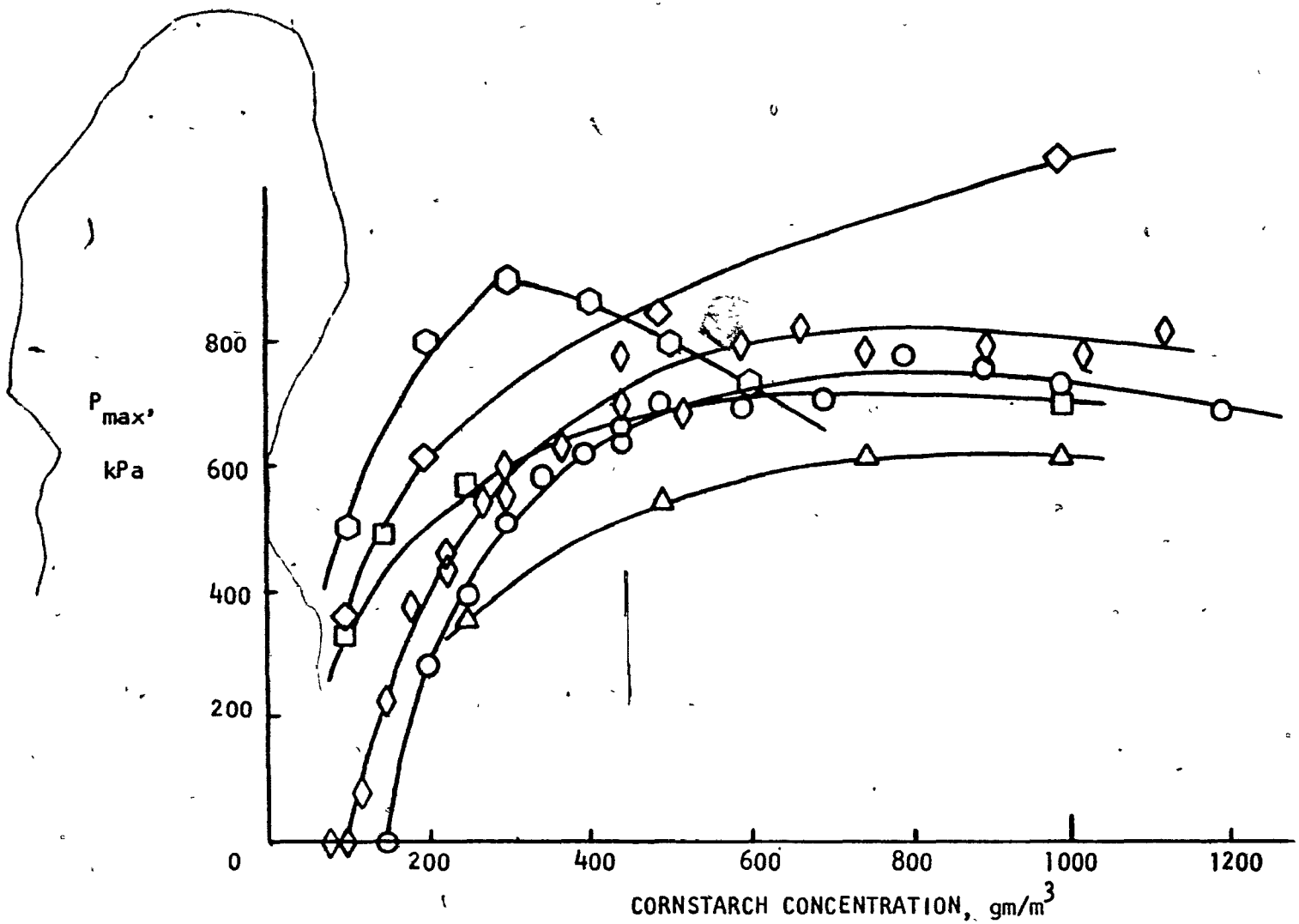

FIGURE 7.- Maximum explosion overpressure versus cornstarch concentration. ◇ McGill 0.333 m^3. ○ McGill 0.180 m^3. △ Cocks and Meyer 0.020 m^3. ◇ Hartmann 0.00123 m^3. □ Nagy 0.00123 m^3. ⬡ Theoretical value calculated from NASA code for adiabatic combustion.

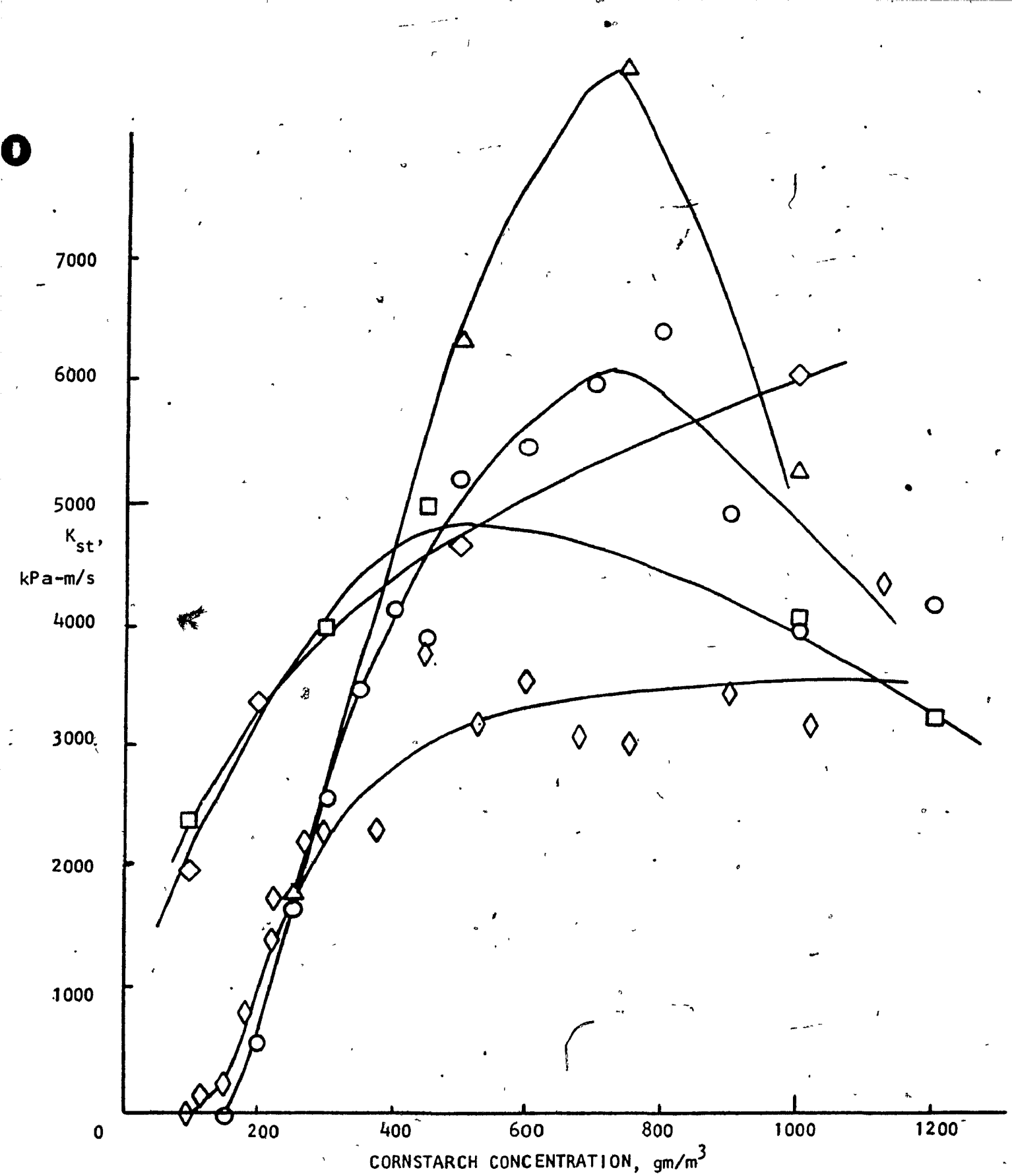

FIGURE 8 - K_{st} versus cornstarch concentration. ◇ McGill 0.333 m^3. ○ McGill 0.180 m^3. △ Cocks and Meyer 0.020 m^3. ◇ Hartmann 0.00123 m^3. □ Nagy 0.00123 m^3.

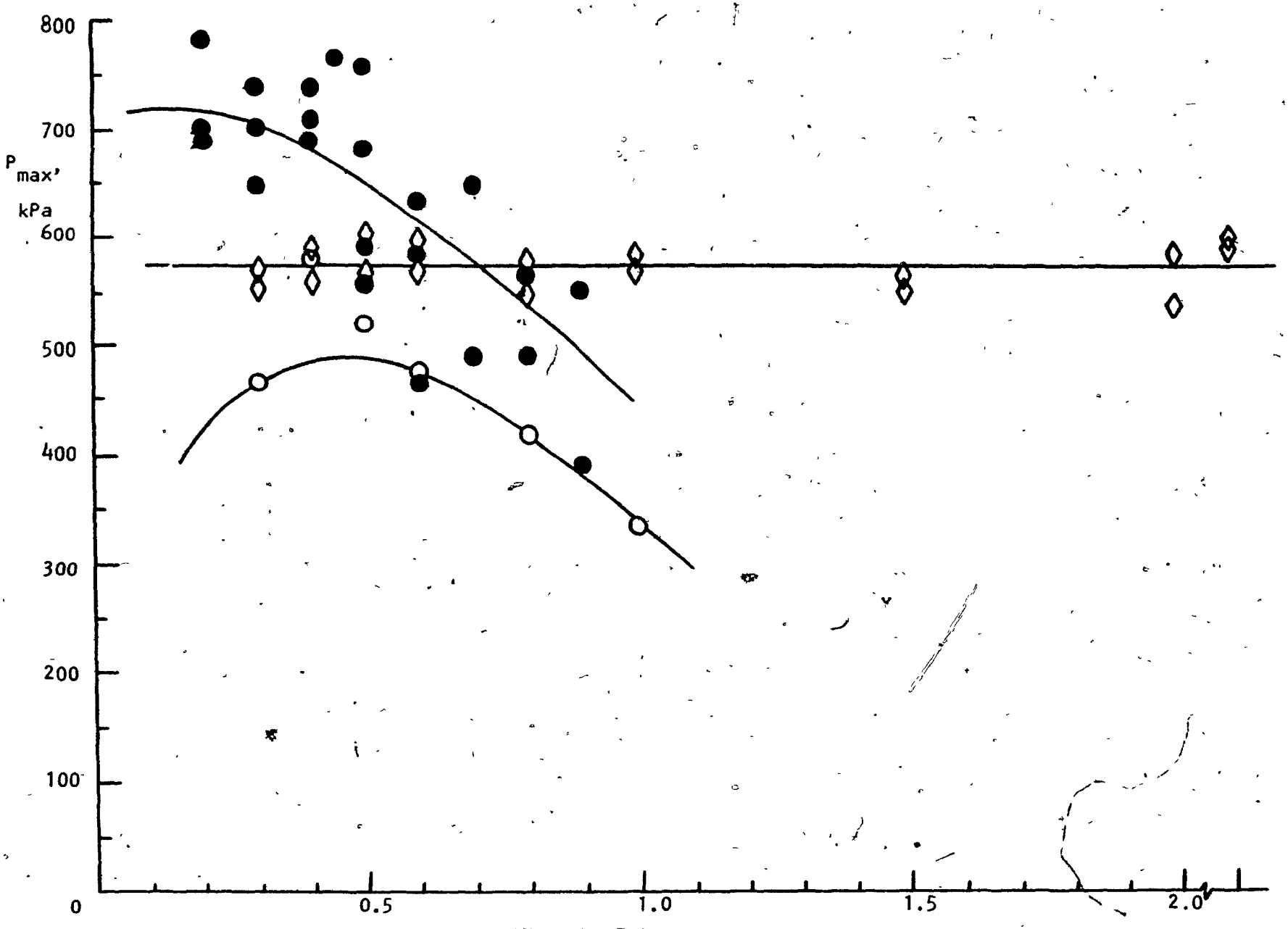

FIGURE 9 - Variation of maximum explosion pressure with ignition delay. ● 450 gm/m^3 starch-air in 333 liter sphere. ◇ 7.5% methane-air in 333 liter sphere. ○ 300 gm/m^3 starch-air in 180 liter cylinder.

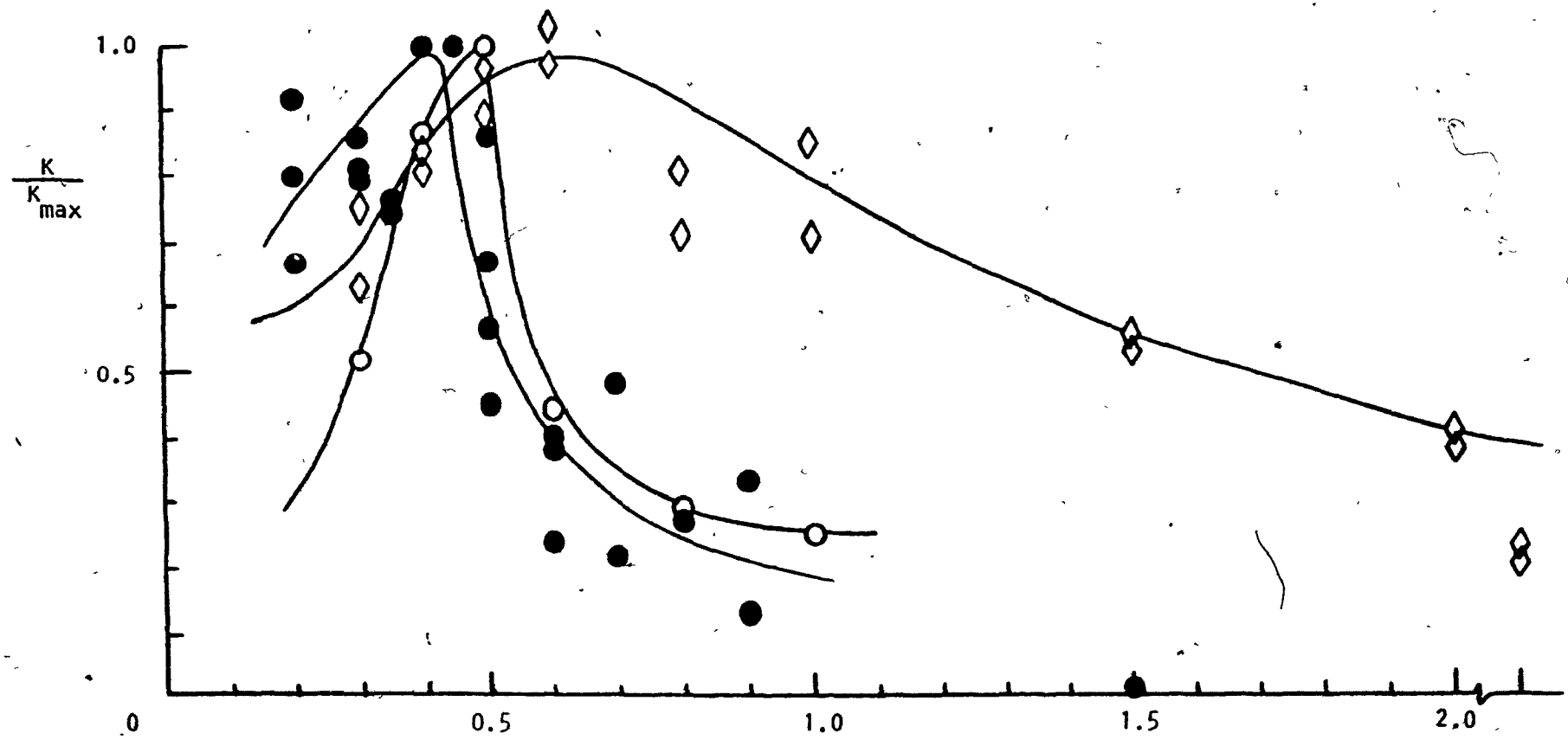

FIGURE 10 - Variation of normalized K factor with ignition delay. ● 450 gm/m^3 starch-air in 333 liter sphere. ◊ 7.5% methane-air in 333 liter sphere. ○ 300 gm/m^3 starch-air in 180 liter cylinder.

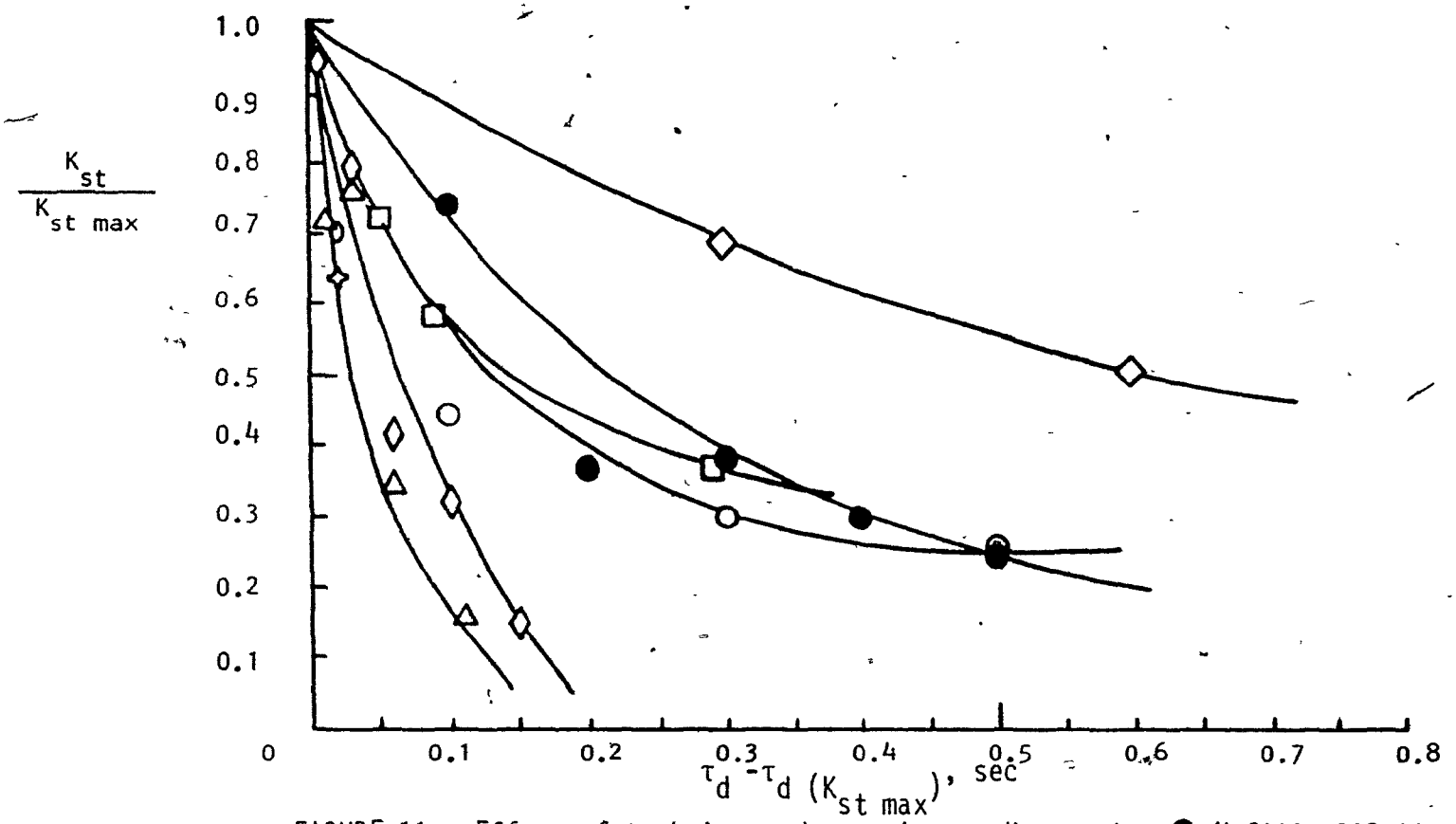

FIGURE 11 - Effect of turbulence decay time on K_{st} ratio. ● McGill, 333 liter sphere (D=0.90 m). ○ McGill, 180 liter cylinder (D=0.50 m). □ Moore, 43 liter sphere (D=0.435 m). ◇ Bartknecht, 1 cu. meter cylinder (D=1.084 m). △ Eckhoff, 1.2 liter cylinder (D=0.07 m). ◊ Moore, 1.75 liter cylinder (D=0.136 m). ✣ Cocks and Meyer, 20 liter sphere (D=0.337 m). O Swift, 26 liter sphere (D=0.368 m).

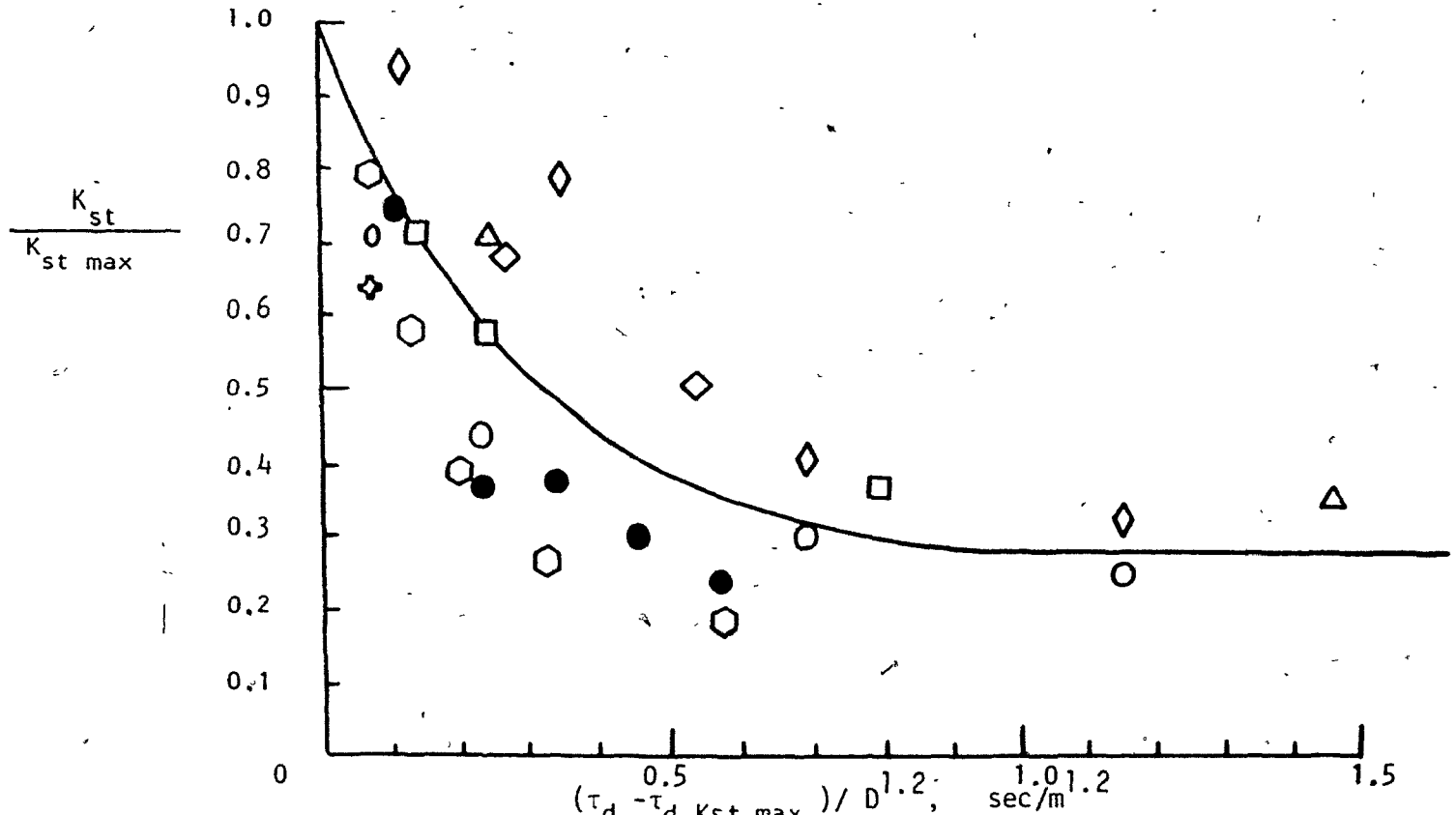

FIGURE 12 - Effect of normalized turbulence decay time on K_{st} ratio. ● McGill, 333 liter sphere (D=0.90 m). O McGill, 180 liter cylinder (D=0.50 m). □ Moore, 43 liter sphere (D=0.435 m). ◇ Bartknecht, 1 cu. meter cylinder (D=1.084 m). △ Eckhoff, 1.2 liter cylinder (D=0.07 m). ◊ Moore, 1.75 liter cylinder (D=0.136 m). ✧ Cocks and Meyer, 20 liter sphere (D=0.337 m). 0 Swift, 26 liter sphere (D=0.368 m). ⬡ Reeh, 115 liter cylinder (D=0.46 m).

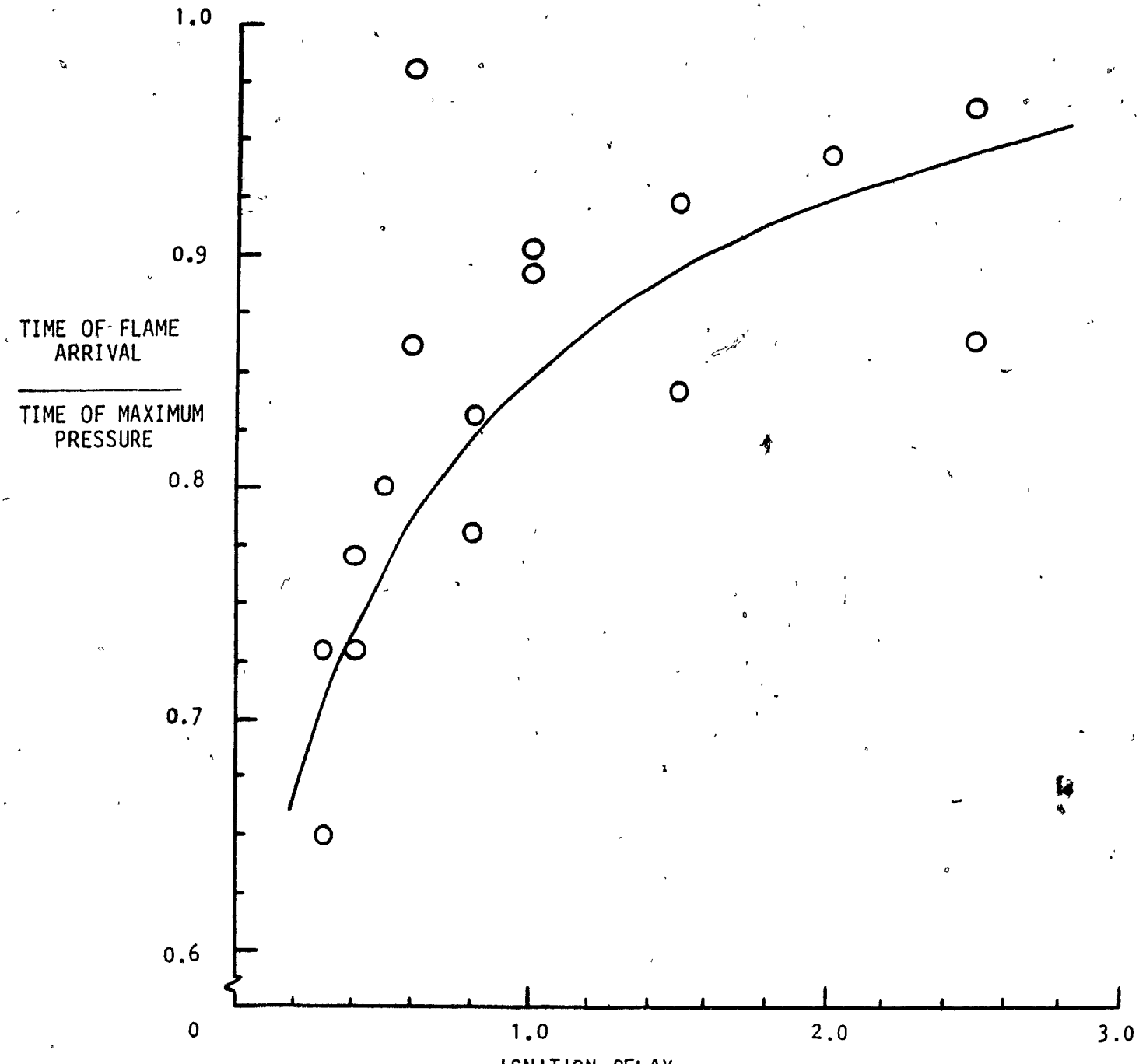

FIGURE 13 - Comparison of Time of flame arrival and time of maximum pressure for 7.5% methane-air explosions with varying ignition delay.

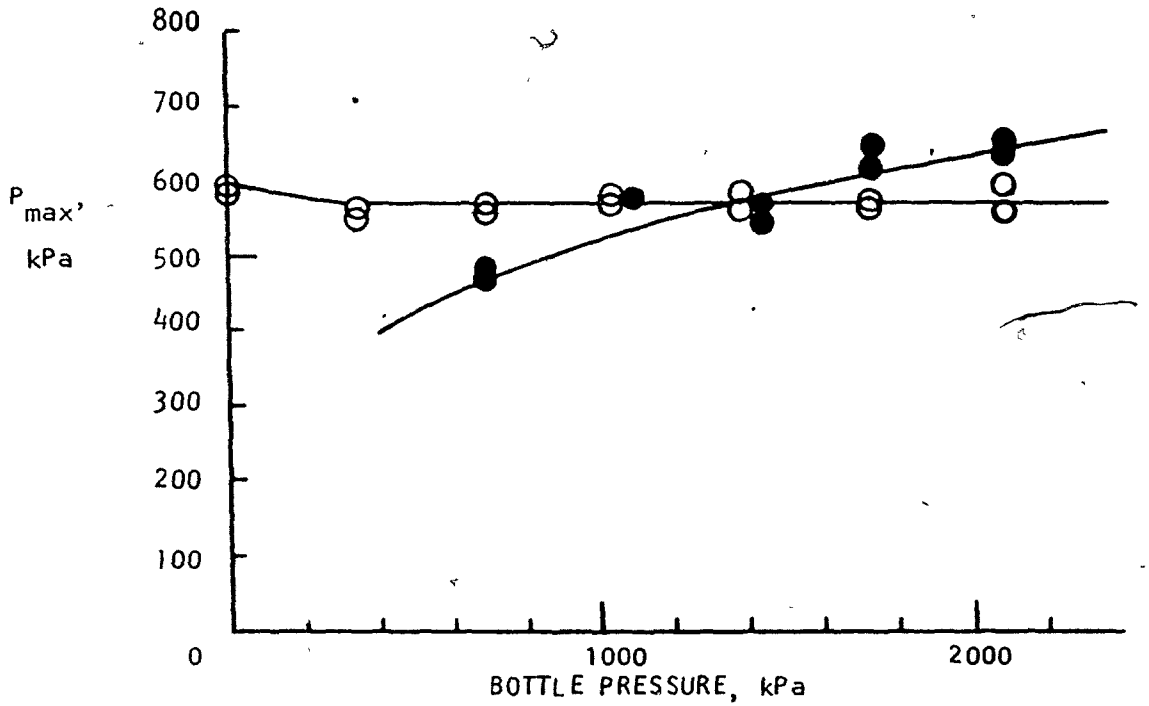

FIGURE 14 - Effect of dispersion bottle pressure on P_{max} in the 333 liter spherical vessel. ○ 7.5% methane-air. ● 300 gm/m^3 cornstarch-air.

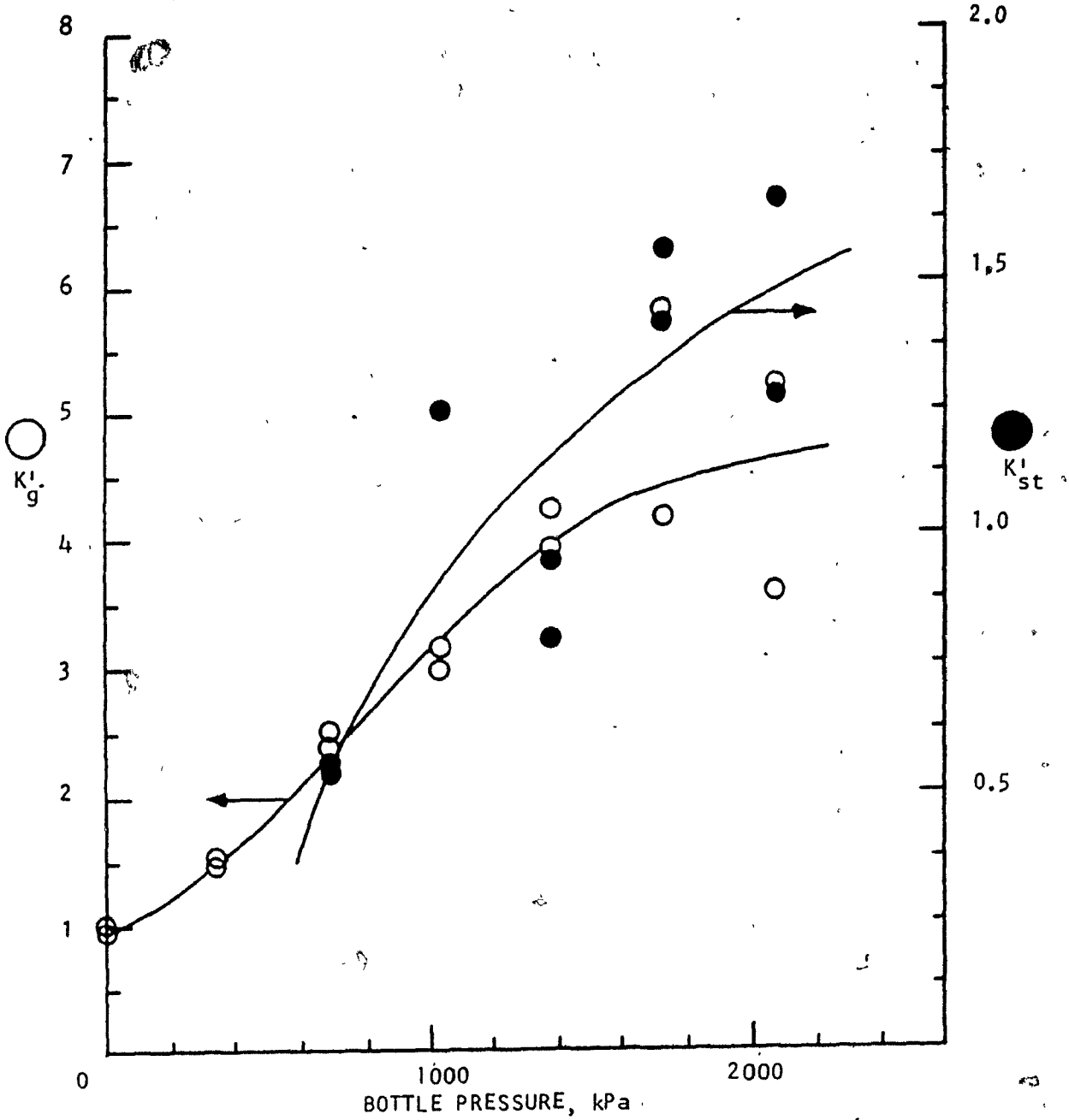

FIGURE 15 - Effect of dispersion bottle pressure on maximum burning rates in 333 liter spherical vessel. ○ 7.5% methane-air. ● 300 gm/m^3 cornstarch-air.

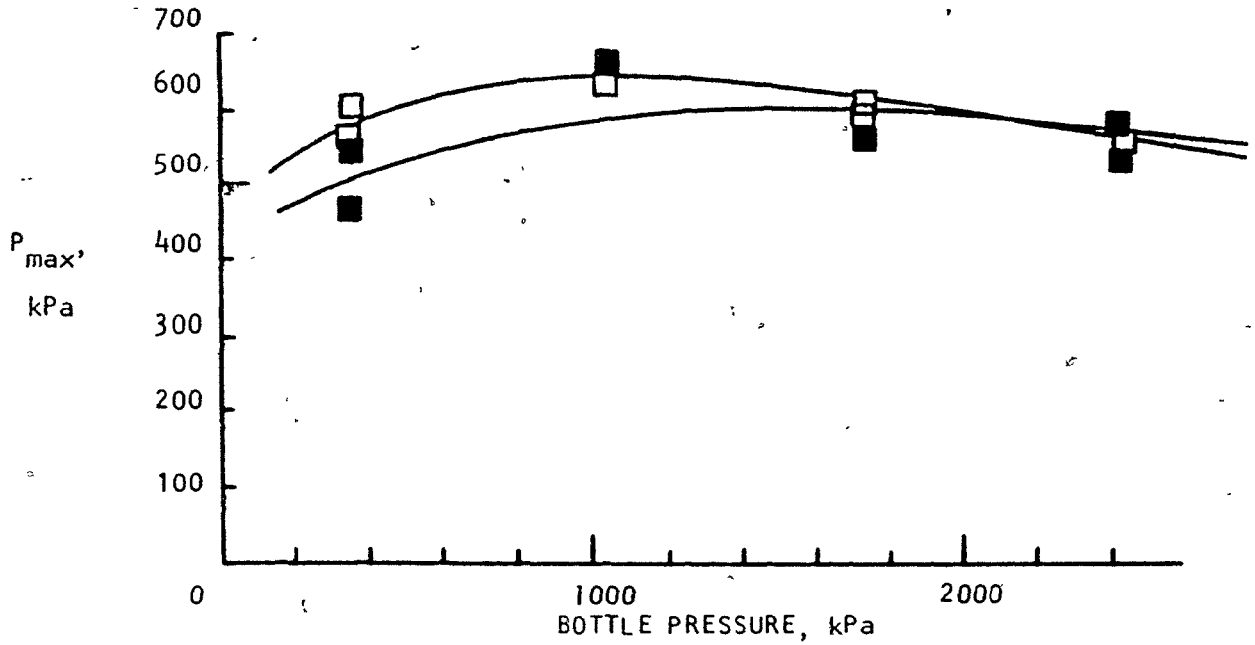

FIGURE 16 - Effect of bottle pressure on P_{max} in 180 liter cylindrical vessel. □ 7.5% methane-air. ■ 300 gm/m^3 cornstarch-air.

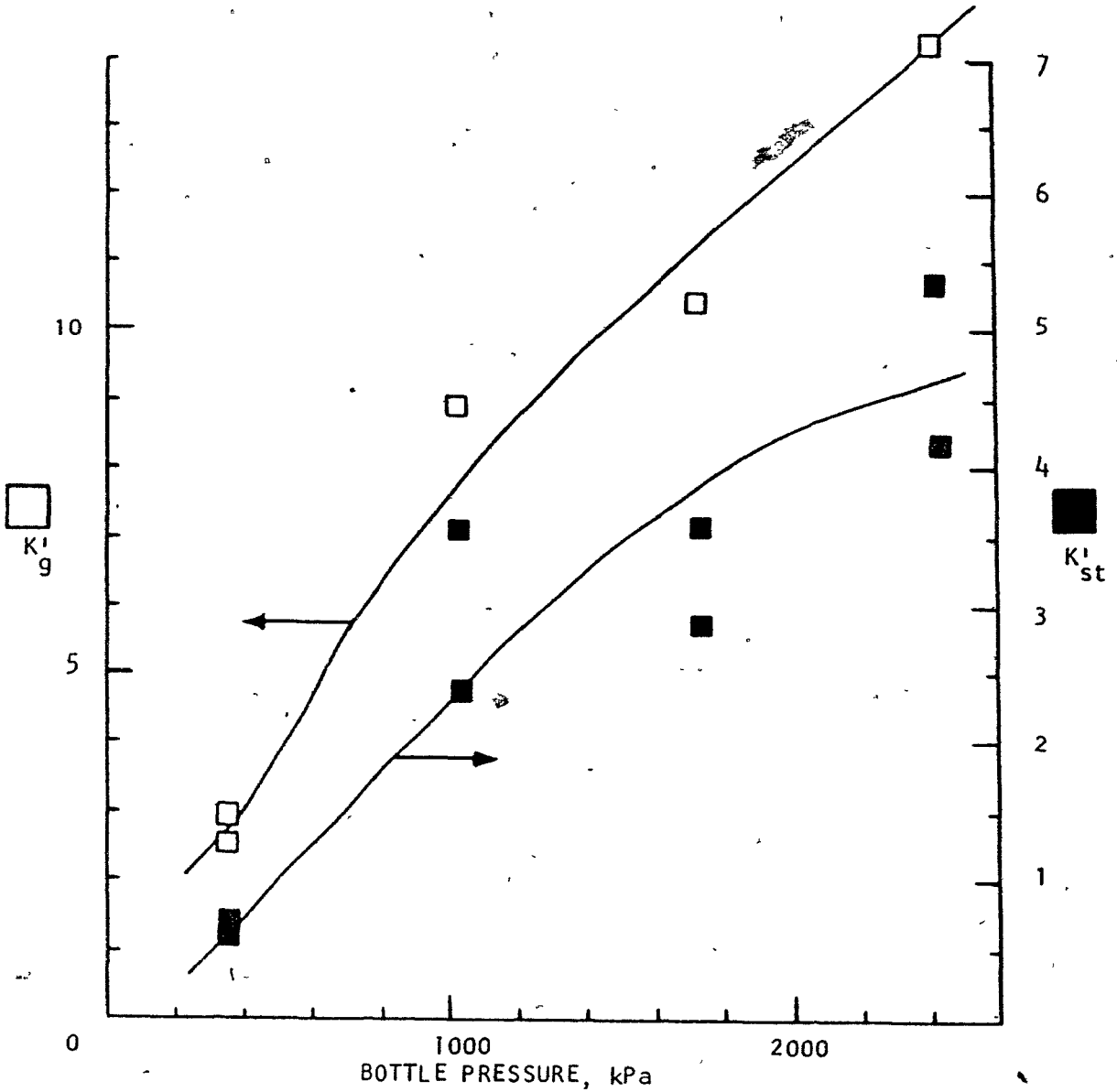

FIGURE 17 - Effect of bottle pressure on maximum burning rates in the 180 liter cylindrical vessel. □ 7.5% methane-air. ■ 300 gm/m^3 cornstarch-air.

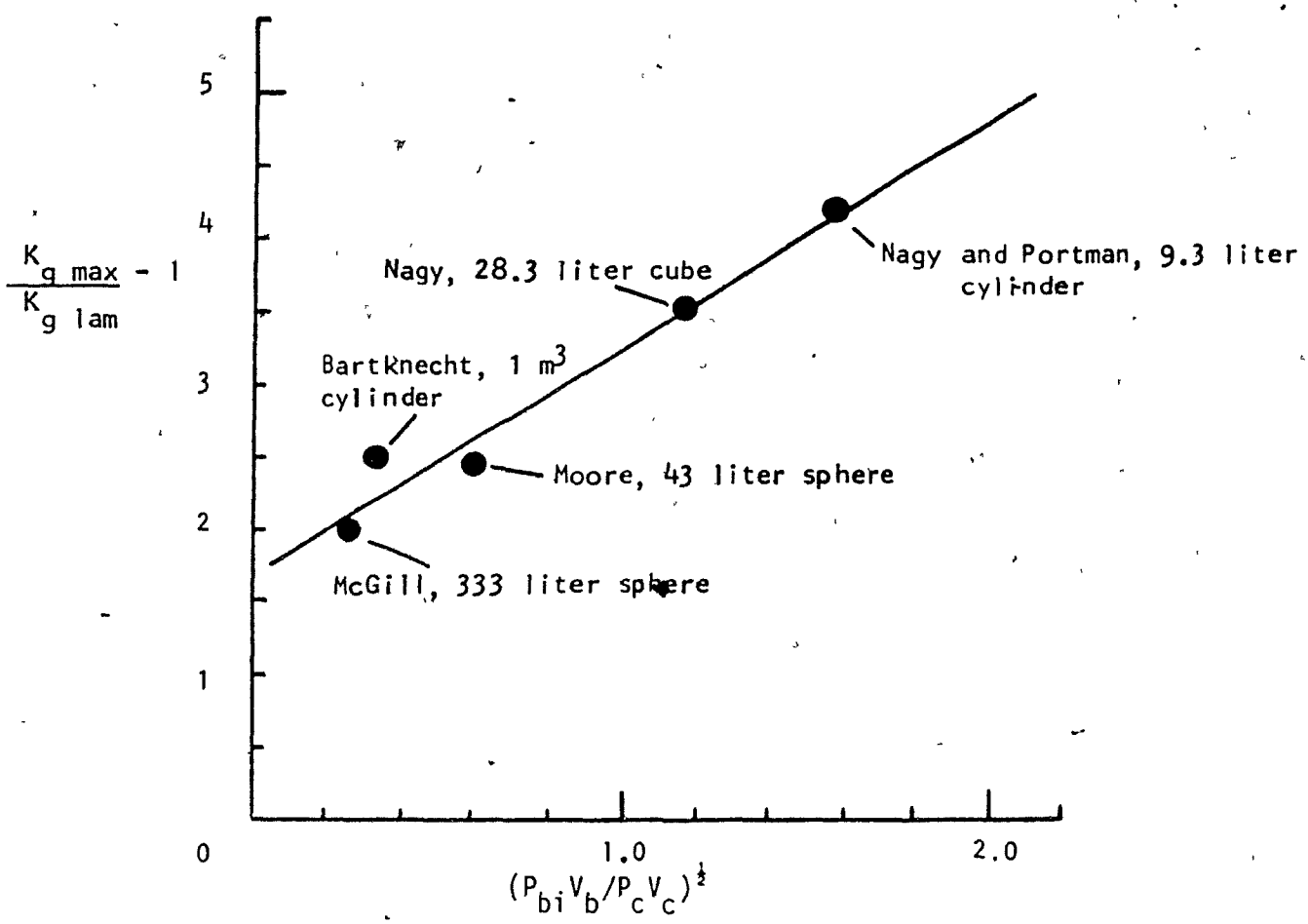

FIGURE 18 - Effect of dispersion characteristics on maximum K_g factor observed in gas-air experiments.

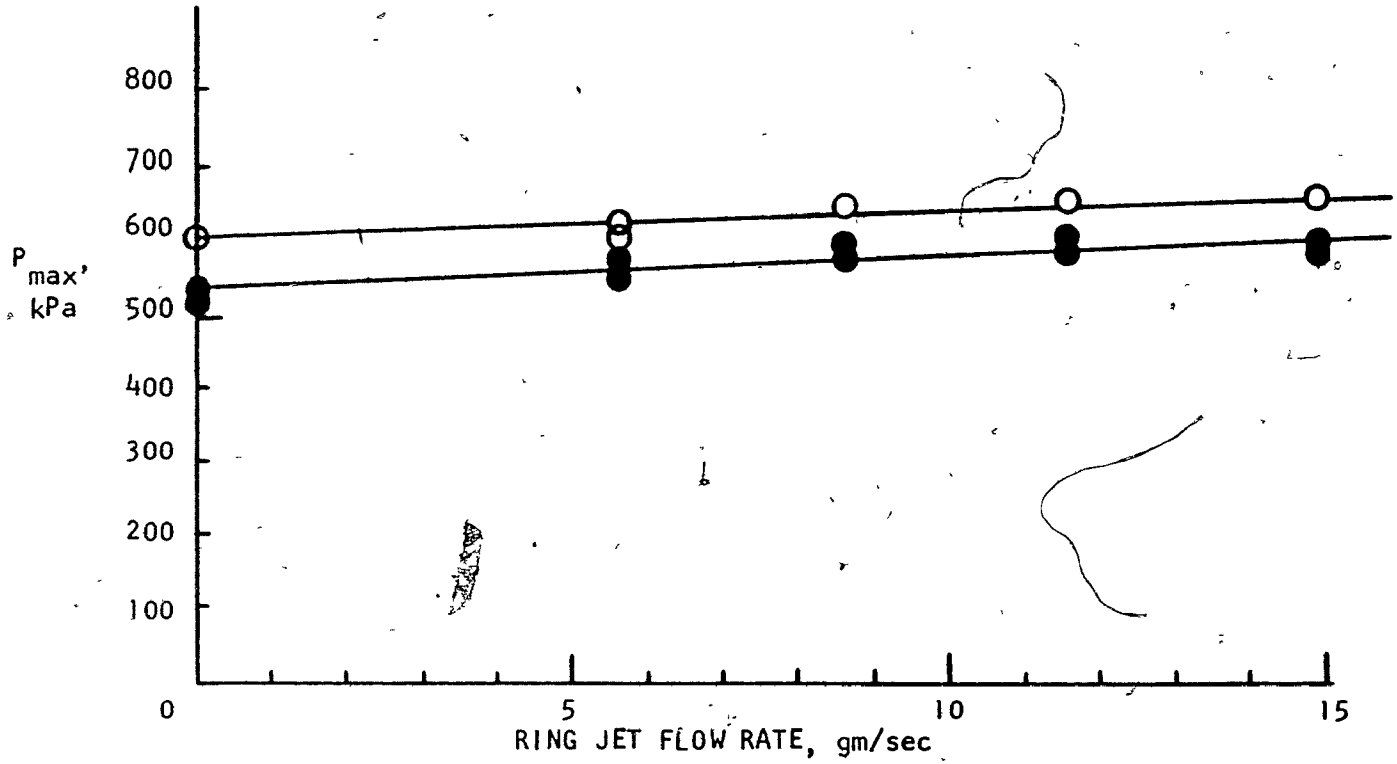

FIGURE 19 - Effect of ring jet flow rate on P_{max} in 7.5% methane-air explosions in the 333 liter spherical vessel. ● with dispersion blast. ○ without dispersion blast.

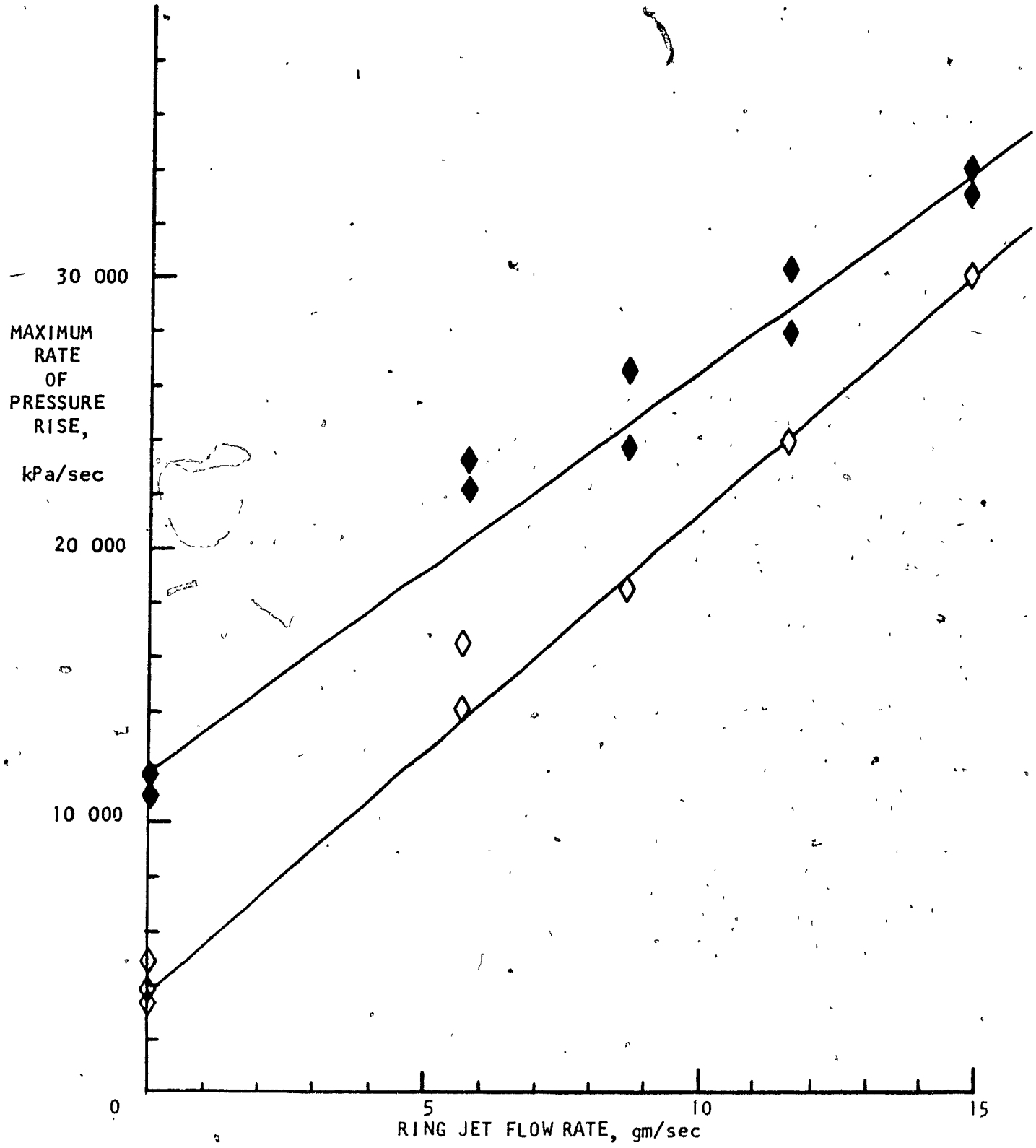

FIGURE 20 - Effect of ring jet flow rate on maximum rate of pressure rise in 7.5% methane-air explosions in the 333 liter spherical vessel. ♦ with dispersion blast. ◊ without dispersion blast.

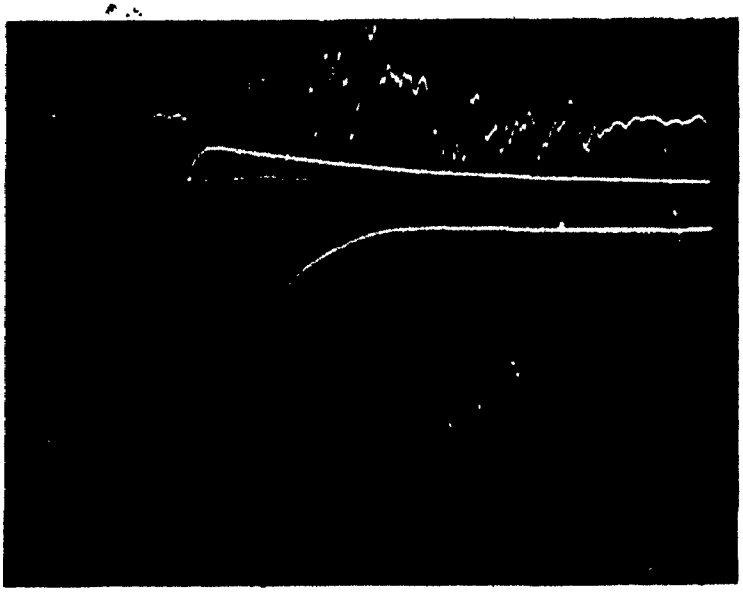

FIGURE 21a - Scope record of 7.5% methane-air explosion with ring jets, without dispersion blast.

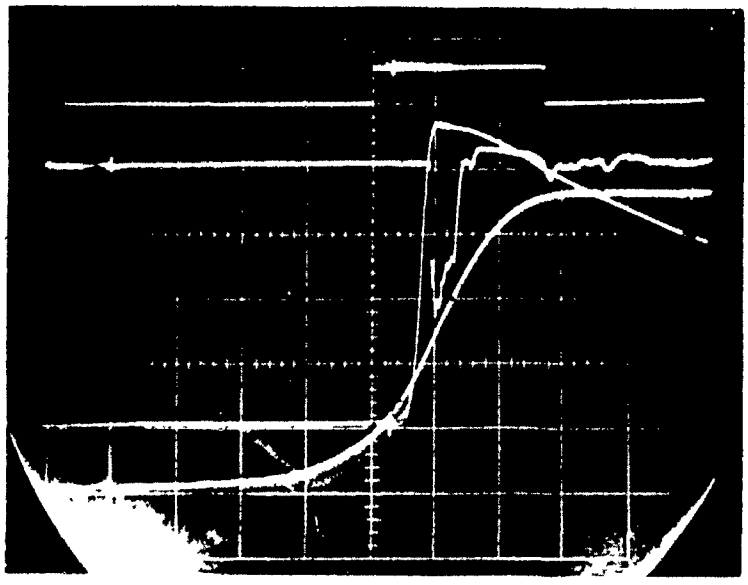

Figure 21b - Scope record of 7.5% methane-air explosion with ring jets, with dispersion blast.

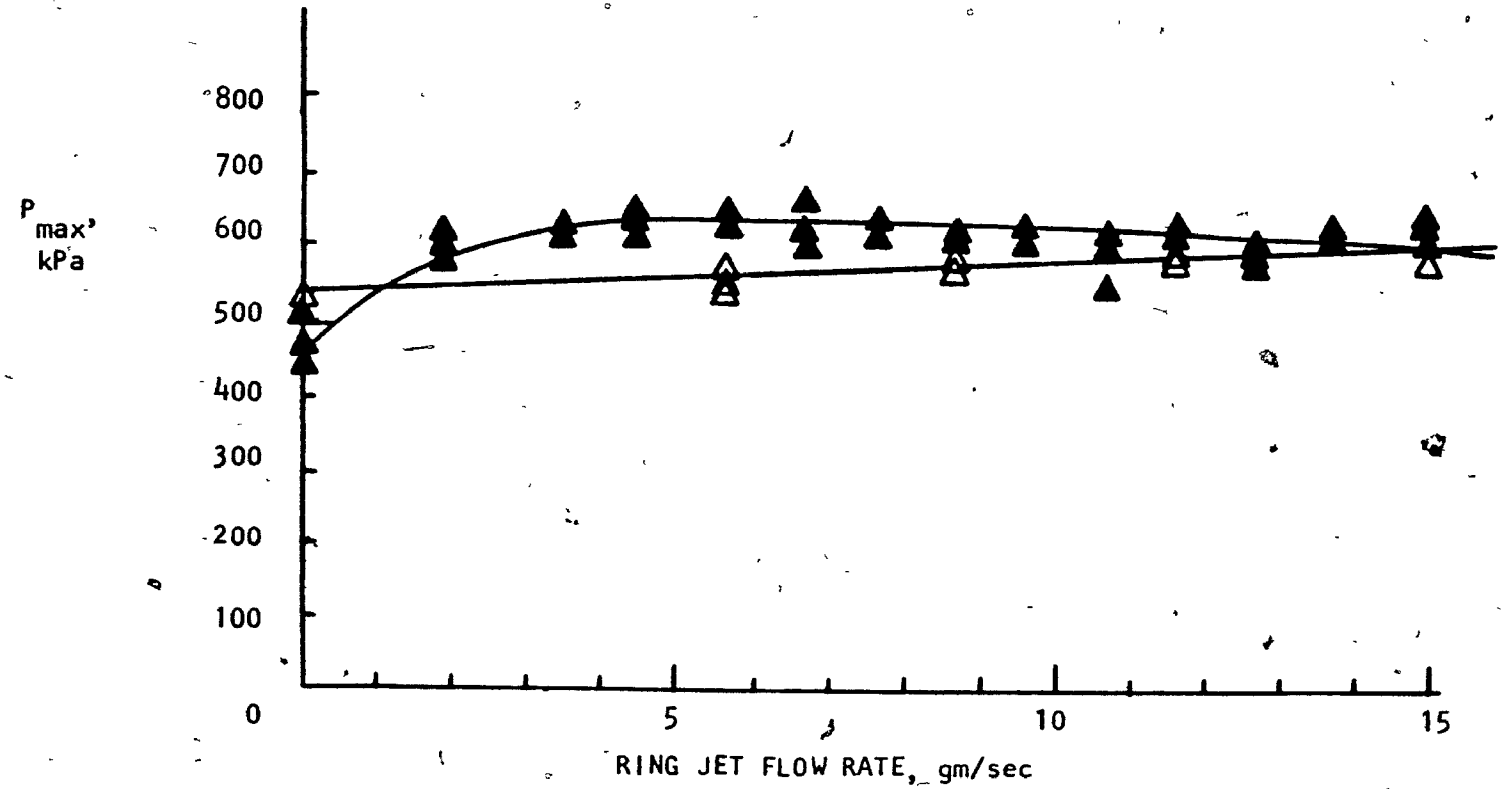

FIGURE 22 - Effect of ring jet flow rate on P_{max} in the 333 liter spherical vessel. △ 7.5% methane-air. ▲ 300 gm/m^3 cornstarch-air.

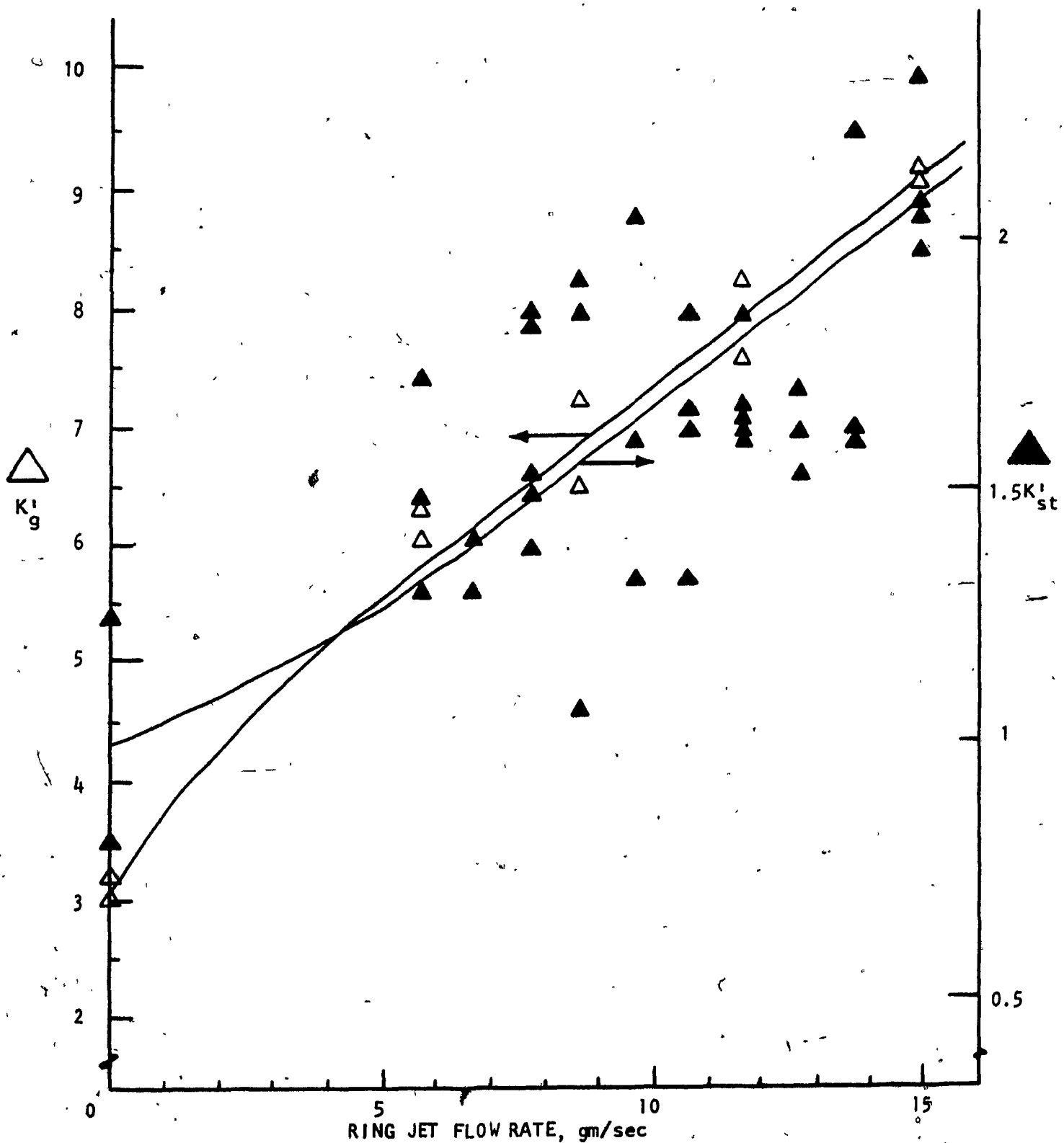

FIGURE 23 - Effect of air mass flow rate through the turbulence ring on the maximum burning rates in the 333 liter spherical vessel. △ 7.5% methane-air. ▲ 300 gm/m^3 cornstarch-air.

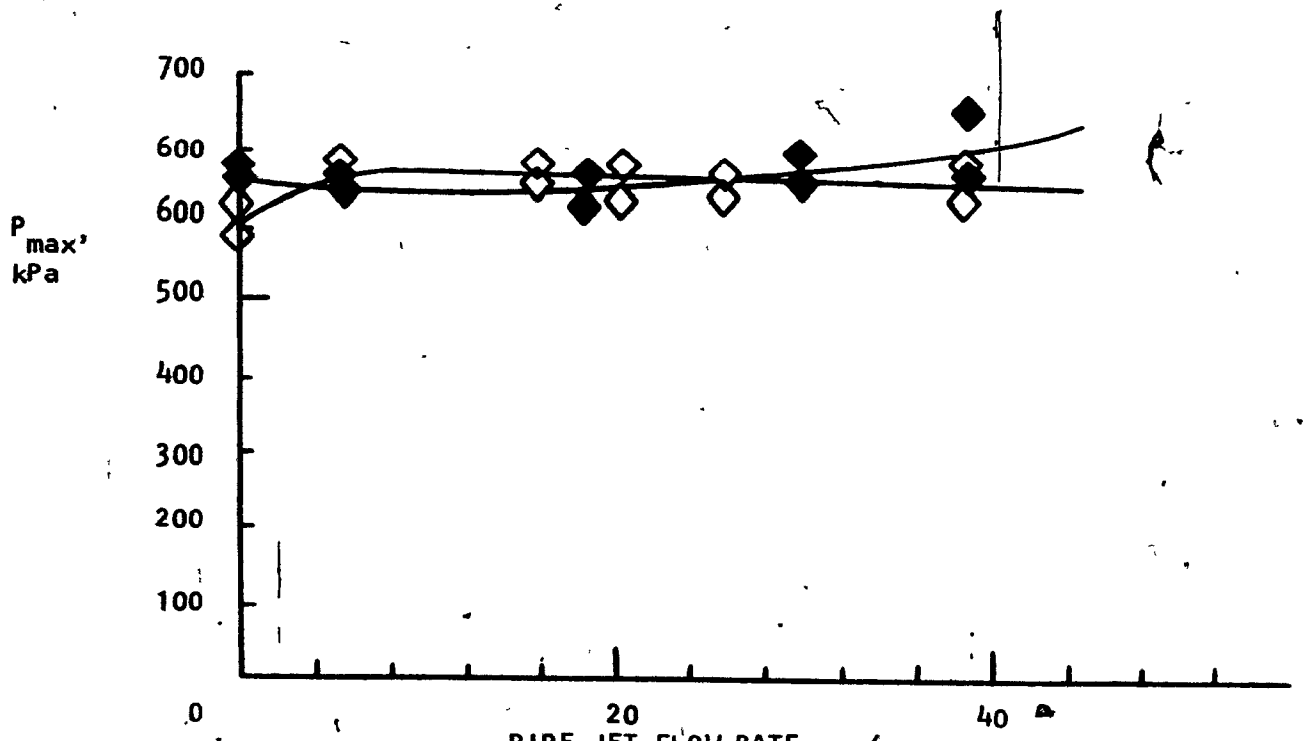

FIGURE 24 - Effect of pipe jet flow rate on P_{max} in the 333 liter spherical vessel. ◇ 7.5% methane-air. ◆ 300 gm/m^3 cornstarch-air.

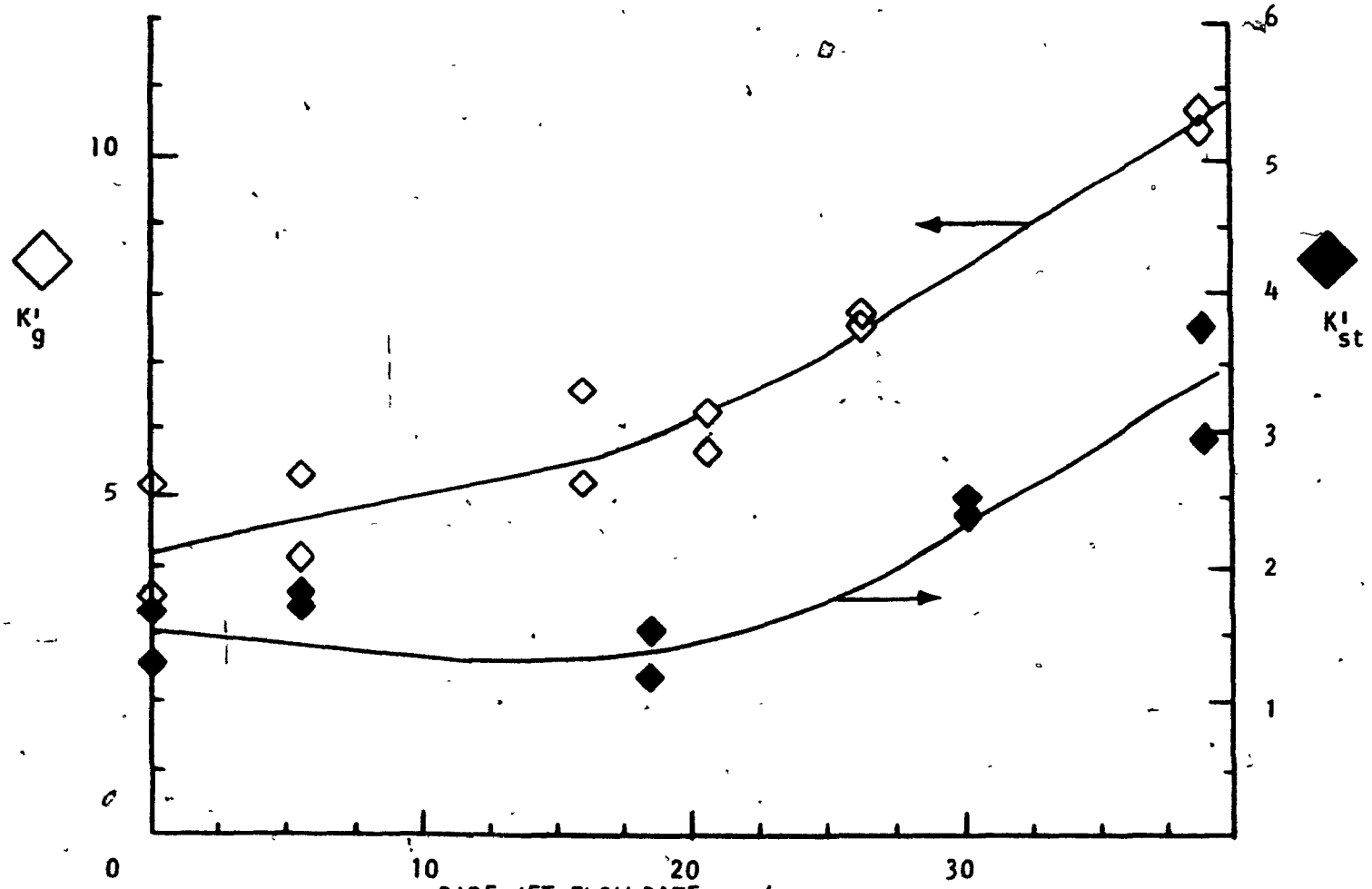

FIGURE 25 - Effect of pipe jet flow rate on the maximum burning rates in the 333 liter spherical vessel. ◇ 7.5% methane-air. ◆ 300 gm/m^3 cornstarch-air.

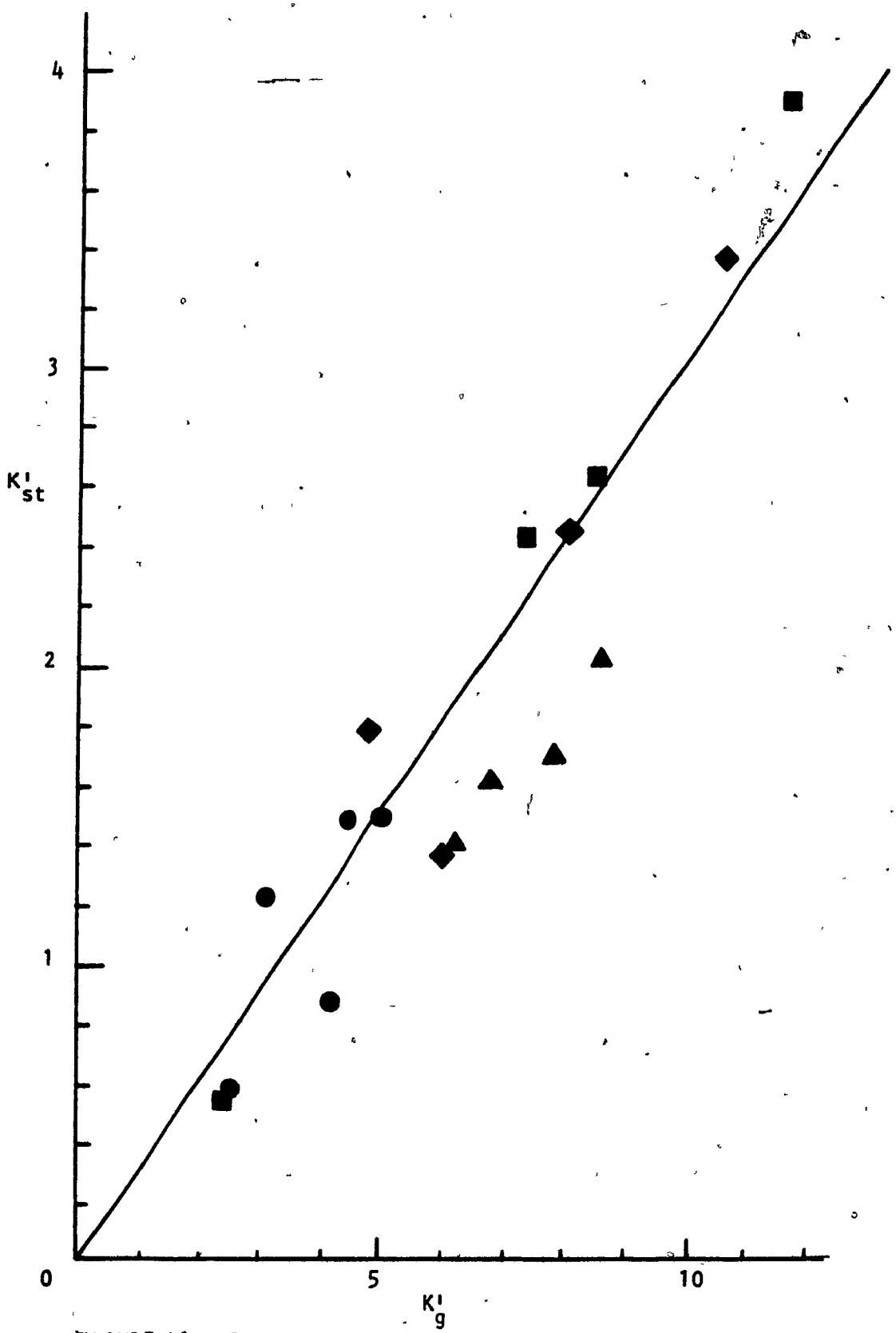

FIGURE 26 - Relationship between dust burning rate and methane burning rate in identical turbulent flow situations. ● Dispersion pressure in 333 liter sphere. ■ Bottle pressure in 180 liter cylinder. ◆ Turbulence pipe in 333 liter sphere. ▲ Turbulence ring in 333 liter sphere.

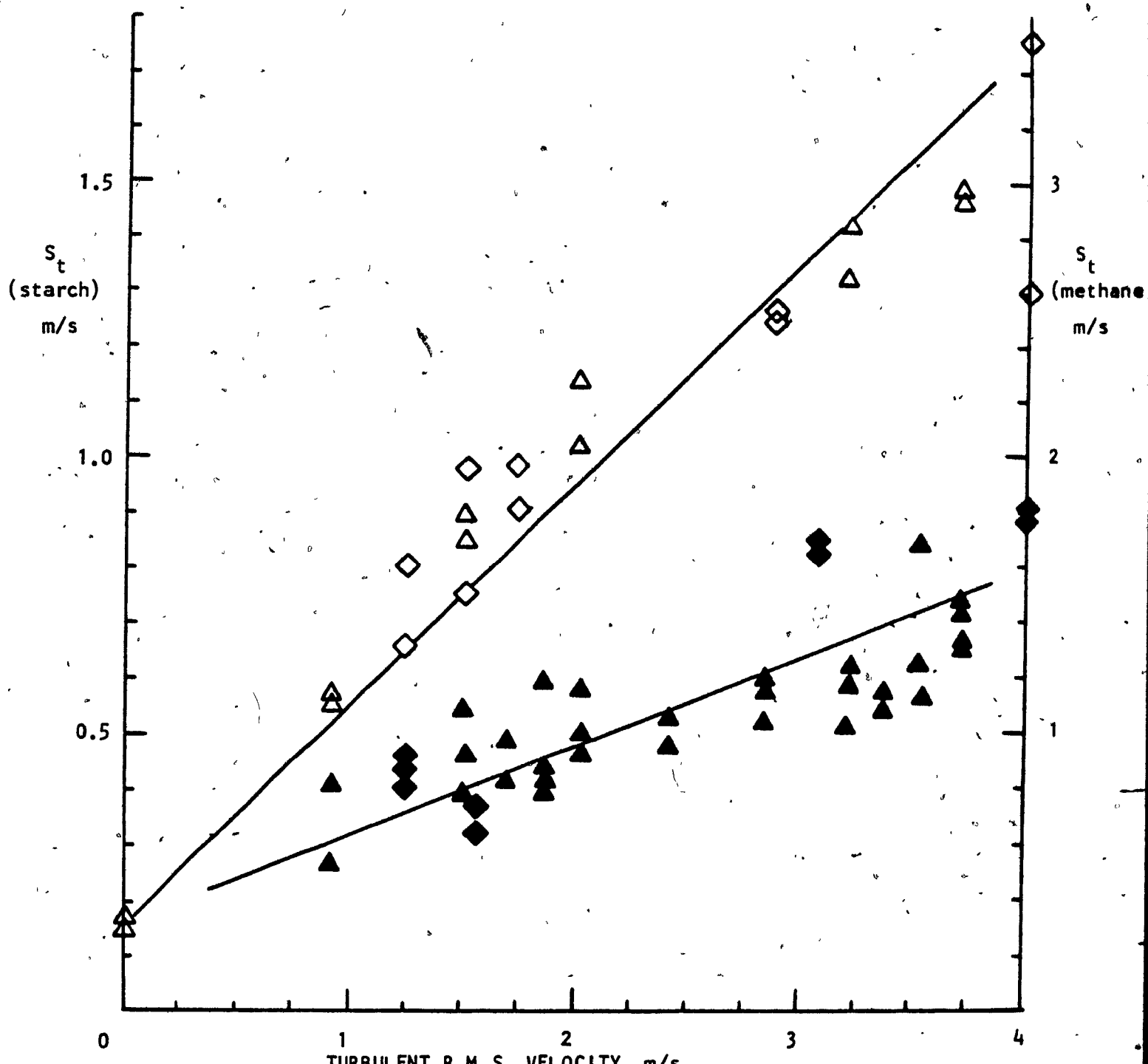

FIGURE 27 - Variation of turbulent burning velocity with turbulent r.m.s. velocity, for starch and methane explosions in 333 liter spherical vessel with jet-induced turbulence. ◇ 7.5% methane-air. ◆ 300 gm/m^3 cornstarch-air. (pipe-induced turbulence) △ 7.5% methane-air. ▲ 300 gm/m^3 cornstarch-air. (ring-induced turbulence).